A novel phenolic derivative inhibits AHL-dependent Quorum Sensing signaling in Pseudomonas aeruginosa

Giulia Bernabè[1], Giovanni Marzaro[2], Giuseppe Di Pietra[1], Ana Otero[3], Massimo Bellato[4], Anthony Pauletto[1], Melania Scarpa[5], Stefania Sut[2], Adriana Chilin[2], Ignazio Castagliuolo[2], Paola Brun[1*], Ignazio Castagliuolo[1]

[1]Department of Molecular Medicine, University of Padova, Italy, [2]Department of Pharmaceutical and Pharmacological Sciences, University of Padova, Italy, [3]Departamento de Microbioloxía e Parasitoloxía, Facultade de Bioloxía-CIBUS, Universidade de Santiago de Compostela, Santiago de Compostela, Spain, Spain, [4]University of Padova, Department of Information Engineering, Italy, [5]Laboratory of Advance Translational Research, Veneto Institute of Oncology IOV-IRCCS, Italy

Submitted to Journal:
Frontiers in Pharmacology

Specialty Section:
Pharmacology of Infectious Diseases

Article type:
Original Research Article

Manuscript ID:
996871

Received on:
18 Jul 2022

Revised on:
02 Sep 2022

Journal website link:
www.frontiersin.org

Conflict of interest statement

The authors declare that the research was conducted in the absence of any commercial or financial relationships that could be construed as a potential conflict of interest

Author contribution statement

GB, PB, IC designed the experiments, interpreted the data, and wrote the paper; GB, SS, SDA ran most of the experiments; GM performed the modeling analysis, GDP isolated and characterized clinical isolates; SS and SDA performed and interpreted the HPLC analysis.

Keywords

Biofilm, antibiotic resistance, Virulence, Quorum sensing inhibitors, molecular docking

Abstract

Word count: 242

Increasing antibiotic resistance and the decline in the pharmaceutical industry's investments have amplified the need for novel treatments for multidrug-resistant bacteria. Quorum sensing (QS) inhibitors reduce pathogens' virulence without selective pressure on bacteria and provide an alternative to conventional antibiotic-based therapies. P. aeruginosa uses complex QS signaling to control virulence and biofilm formation. We aimed to identify inhibitors of P. aeruginosa QS acting on acyl-homoserine lactones (AHL)-mediated circuits. Bioluminescence and qRT-PCR assays were employed to screen a library of 81 small phenolic derivatives to reduce AHL-dependent signaling. We identified GM-50 as the most active compound inhibiting the expression of AHL-regulated genes but devoid of cytotoxic activity in human epithelial cells and biocidal effects on bacteria. GM-50 reduces virulence factors such as rhamnolipids, pyocyanin, elastase secretion, and swarming motility in P. aeruginosa PAO1 laboratory strain. By molecular docking, we provide evidence that GM-50 highly interacts with RhlR. GM-50 significantly improved aztreonam-mediated biofilm disruption. Moreover, GM-50 prevents adhesion of PAO1 and inflammatory damage in the human A549 cell line and protects Galleria mellonella from PAO1-mediated killing. GM-50 significantly reduces virulence factors in 20 P. aeruginosa clinical isolates from patients with respiratory tract infections.

In conclusion, GM-50 inhibits AHL-signaling, reduces virulence factors, enhances the anti-biofilm activity of aztreonam, and protects G. mellonella larvae from damage induced by P. aeruginosa. Since GM-50 is active on clinical strains, it represents a starting point for identifying and developing new phenolic derivatives acting as QS-inhibitors in P. aeruginosa infections.

Contribution to the field

The antibiotic resistance during infections by Pseudomonas aeruginosa is a global health and development threat that requires urgent multidisciplinary actions. In our original research study, we screened a library of new compounds as promising inhibitors of the Quorum Sensing of P. aeruginosa. In vitro experiments validated the anti-virulence effects of a compound against laboratory strain and clinical isolates of P. aeruginosa obtained from patients suffering from airway infections. Moreover, we reported that the Quorum sensing inhibitor in association with antibiotics successfully disrupt P. aeruginosa biofilm. Finally, using molecular docking approach, we identified that the inhibitor is selective for the Rhl system of the Quorum Sensing in P. aeruginosa. The inhibition of the Rhl pathway is sufficient to shut down the virulence of the bacterium and dampen the inflammation in eukaryotic. The results of our original study shed light on the role of Rhl pathway in pathogenicity of P. aeruginosa and advance the research in the use of inhibitors for specific pathways of the Quorum Sensing system. The association of traditional antibiotics with novel antivirulence agents represents an approach to reevaluate the use of antibacterial agents in the antibiotic resistance era.

Funding statement

The funding agencies had no role in study design, data collection, interpretation, or the decision to submit the manuscript for publication.

Ethics statements

Studies involving animal subjects
Generated Statement: No animal studies are presented in this manuscript.

Studies involving human subjects
Generated Statement: No human studies are presented in this manuscript.

Inclusion of identifiable human data
Generated Statement: No potentially identifiable human images or data is presented in this study.

Data availability statement

Generated Statement: The original contributions presented in the study are included in the article/supplementary material, further inquiries can be directed to the corresponding author/s.

A novel phenolic derivative inhibits AHL-dependent Quorum Sensing signaling in *Pseudomonas aeruginosa*

Giulia Bernabè[1], Giovanni Marzaro[2], Giuseppe Di Pietra[1], Ana Otero[3], Massimo Bellato[4], Anthony Pauletto[1], Melania Scarpa[5], Stefania Sut[2], Adriana Chilin[2], Stefano Dall'Acqua[2], Paola Brun[1*], Ignazio Castagliuolo[1*]

[1]Department of Molecular Medicine, University of Padua, Padua, Italy
[2]Department of Pharmaceutical and Pharmacological Sciences, University of Padua, Padua, Italy
[3]Departamento de Microbioloxía e Parasitoloxía, Facultade de Bioloxía-CIBUS, Universidade de Santiago de Compostela, Santiago de Compostela, Spain
[4]Department of Information Engineering, University of Padua, Padua, Italy
[5]Laboratory of Advanced Translational Research, Veneto Institute of Oncology IOV - IRCCS, Padua, Italy
*These authors have contributed equally to the work and share last authorship

Corresponding author
Paola Brun
Department of Molecular Medicine
University of Padova, Italy
E-mail: paola.brun.1@unipd.it

Number of words: 7975
Number of figures: 12
Number of tables: 2

Abstract

Increasing antibiotic resistance and the decline in the pharmaceutical industry's investments have amplified the need for novel treatments for multidrug-resistant bacteria. Quorum sensing (QS) inhibitors reduce pathogens' virulence without selective pressure on bacteria and provide an alternative to conventional antibiotic-based therapies. *P. aeruginosa* uses complex QS signaling to control virulence and biofilm formation. We aimed to identify inhibitors of *P. aeruginosa* QS acting on acyl-homoserine lactones (AHL)-mediated circuits. Bioluminescence and qRT-PCR assays were employed to screen a library of 81 small phenolic derivatives to reduce AHL-dependent signaling. We identified GM-50 as the most active compound inhibiting the expression of AHL-regulated genes but devoid of cytotoxic activity in human epithelial cells and biocidal effects on bacteria. GM-50 reduces virulence factors such as rhamnolipids, pyocyanin, elastase secretion, and swarming motility in *P. aeruginosa* PAO1 laboratory strain. By molecular docking, we provide evidence that GM-50 highly interacts with RhlR. GM-50 significantly improved aztreonam-mediated biofilm disruption. Moreover, GM-50 prevents adhesion of PAO1 and inflammatory damage in the human A549 cell line and protects *Galleria mellonella* from PAO1-mediated killing. GM-50 significantly reduces virulence factors in 20 *P. aeruginosa* clinical isolates from patients with respiratory tract infections.
In conclusion, GM-50 inhibits AHL-signaling, reduces virulence factors, enhances the anti-biofilm activity of aztreonam, and protects *G. mellonella* larvae from damage induced by *P. aeruginosa*. Since GM-50 is active on clinical strains, it represents a starting point for identifying and developing new phenolic derivatives acting as QS-inhibitors in *P. aeruginosa* infections.

Keywords: biofilm, antibiotic resistance, virulence, quorum sensing inhibitors, molecular docking

1 Introduction

The misuse of antibiotics has dramatically sped up the spread of multi-drug resistant bacterial pathogens, increasing the occurrence of infections that are challenging to treat (Boucher *et al.*, 2009). Thus, it is not surprising that pharmaceutical companies consider the R&D for new antimicrobial drugs less attractive than other therapeutic areas – i.e., neurodegenerative diseases, cancer, and metabolic diseases. Although developing a novel antibiotic needs significant investments, the economic reward is uncertain because of the unsure commercial life of antimicrobial drugs due to the possible rapid emergence of resistant strains (Luepke *et al.*, 2017). Moreover, the ongoing pandemic of coronavirus disease may have a complex long-term impact on antibacterial resistance (Rawson *et al.*, 2020). A very recent study reported an odd use of broad-spectrum antimicrobials compared to a low incidence of bacterial infection in hospitalized COVID-19 patients (Lansbury *et al.*,2020). Thus, the COVID-19 pandemic causes unnecessary antimicrobial use and possibly boosts multidrug-resistant (MDR) bacteria (Rawson *et al.*, 2020).
As the antibacterial effects of antibiotics are associated with selective pressure and the occurrence of resistance, virulence mechanisms have been pointed out as molecular targets for novel drugs since they should hamper the infection process, avoiding effects on bacterial growth (Maura *et al.*, 2016;

Montserrat-Martinez *et al.*, 2019). Quorum Sensing (QS) signaling controls bacterial virulence and provides an ideal target for developing a new class of antibacterial molecules. QS is a cell-to-cell communication system by which bacteria harmonize the expression of virulence factors and tune their behaviors based on bacterial population density and the release/reception of signal molecules (Kalia *et al.*, 2019).

Pseudomonas aeruginosa (PA) has been listed among the MDR nosocomial pathogens that require new therapeutic strategies. The last report of the European Antimicrobial Surveillance pointed out that 31.8% of PA clinical isolates are resistant to at least one of the antibiotic groups under surveillance (EARS-net, 2020). In Italy, it was observed that in 2018 PA reported the highest resistance to piperacillin-tazobactam (23.9%), fluoroquinolones (22.9%), ceftazidime (19.9%), carbapenems (15.8%), and aminoglycosides (13.7%) (Bellino *et al.*, 2018). Moreover, epidemiological studies have revealed that PA rapidly develops resistance to imipenem, tobramycin, ciprofloxacin, and aztreonam, the first-line antibiotics used to treat PA infections (Obritsch *et al.*, 2004; Hill *et al.*, 2006). PA establishes acute or chronic infections by regulating the expression of metabolic pathways and virulence factors, mainly through QS-signalling (Crousilles *et al.*, 2015). In particular, QS in PA is characterized by at least four circuits deeply interconnected: LasI-LasR, RhlI-RhlR, the quinolone-signal-system, and the IQS circuit. The circuits respectively respond to 3-oxo-*N*-[(3*S*)-2-oxooxolan-3-yl]dodecanamide (3OC12-HSL), *N*-[(3*S*)-2-oxooxolan-3-yl]butanamide (C4-HSL), and 2-heptyl-3-hydroxy-1*H*-quinolin-4-one (PQS) to produce 2-(2-hydroxyphenyl)-1,3-thiazole-4-carbaldehyde (IQS). These QS circuits are hierarchically organized, with the Las system at the top of the cascade (Thi *et al.*, 2020). LasI-LasR system includes LasI synthetase that catalyzes the production of 3-oxo-C12-HSL (AHL) as the signal molecule. Once secreted in the extracellular environment, AHL diffuses inside nearby bacterial cells and binds to the LasR receptor. The AHL-LasR complex activates the expression of target genes coding for LasI-synthetase, LasA and LasB elastases, alkaline protease, and genes of the Rhl and PQS QS systems. In the RhlI-RhlR system, the Rhl-synthetase produces the N-butyryl-L-homoserine-lactone, which diffuses in the extracellular space to enter adjacent cells by diffusion and binds the receptor RhlR. The ligand-receptor complex promotes the production of rhamnolipids, LasB elastase, pyocyanin, hydrogen cyanide, and RhlI (Lee *et al.*, 2014). Blocking the quorum sensing signaling may disarm the pathogen by interfering with the coordinated production of its virulence factors such as toxin production, biofilm organization, or making PA more vulnerable to antibiotics. Specifically, more than 300 genes of PA are regulated by QS, that therefore acquires a critical role in *P. aeruginosa* pathogenicity and drug resistance (Girard *et al.*, 2008). Among innovative molecules showing QS inhibitory activity, phenolic compounds show interesting properties (Hossain *et al.*, 2017; Langendonk *et al.*, 2021). For example, naringenin, a flavonoid QS inhibitor, competes with AHL-induced LasR activation but only at low *P. aeruginosa* population cellular densities, a situation not representative of common clinical infection (Piepenbrink *et al.*, 2020). Moreover, natural phenolic derivatives such as salicylic acid and trans-cinnamaldehyde possess a QS inhibitory activity only at high or toxic concentrations (Ahmed *et al.*, 2019). Therefore, it is desirable to develop novel phenolic derivatives to identify more effective compounds.

In this study, we screened an in-house library of phenolic derivatives to identify novel QS inhibitors in PA. The tested compounds (either monocyclic or bicyclic derivatives) are derived from our extensive works on cumarins and chromones (Guiotto et al., 1984; Rodighiero *et al.*, 1997; Chilin *et al.*, 2008;

Borgatti *et al*., 2011) for whose synthesis the phenols constitute key intermediates. After *in-vitro* experiments, we corroborated our results in the *G. mellonella* larvae infection model. Since PA clinical isolates differ from the laboratory-adapted strain PAO1 for the variability in the phenotype, we tested the most promising antivirulence molecules on 39 PA strains isolated from the respiratory tract of patients with chronic obstructive pulmonary disease (COPD). Overall, the compound GM-50 exhibited the most significant antivirulence activity, enhancing aztreonam efficacy on PA biofilm formation. We deem that this molecule is a starting point to developing a new pharmacophore of QS inhibitors active in *P. aeruginosa* infections.

2. Material and Methods

2.1 Bacterial strains and growth conditions

We used *P. aeruginosa* (Schroeter *et al*., 1872) Migula 1900 (DSM 50071^T) (CCUG241, Culture Collection University of Gothenburg) (Nakano *et al.*, 2015) (PAO1) cultured in Luria-Bertani (LB) broth. Bioluminescence assays for the detection of the production of AHLs by *P. aeruginosa* were conducted with two different *Vibrio harveyi* strains (Henke *et al*., 2004). We used *Vibrio harveyi BB120* (HAI-1 positive; AI-2 positive; CAI-1 negative) and *Vibrio harveyi* JAF548. The last one was used as a negative control since the bioluminescence is not controlled by QS systems due to the permanent activation of LuxO, the QS-dependent bioluminescence repressor (Freeman *et al*., 1999). Both strains were cultured at 30 °C in Marine Agar/Broth pH 7.0 (MA/MB, Difco) and experiments were performed in Autoinducer Bioassay medium (AB, Difco) prepared as described (Greenberg *et al*., 1979).

2.2 Bacterial isolates

Thirty-nine strains of *P. aeruginosa* were isolated from sputum specimens, samples representative of the lower respiratory tract, exanimated, and identified at the Clinical Microbiology Laboratory of Padua University Hospital by MALDI-TOF mass spectrometry. Antibiotic susceptibility was assessed by broth microdilution (BMD) using Sensititre™ Gram Negative Susceptibility Testing Plate (Trek diagnostic system) following Eucast breakpoint 2021.

2.3 Selection of compounds

Based on the recently reported evidence that phenolic (Hossain *et al.*, 2017) and fused phenolic compounds (Langendonk *et al*., 2021) negatively regulate the QS, we tested our in-house library of phenolic derivatives (81 compounds). The library contained monocyclic phenol derivatives and fused polycyclic phenols (cumarines and chromones). Compounds were initially examined for their ability to interfere with the release of AHLs in *P. aeruginosa* planktonic cultures by bioluminescence assay.

2.4 Bioluminescence assay

To screen the effect of compounds on AHL signaling, PAO1 (10^6 CFU/mL) was cultured for 24 hours (hrs) at 37 °C in LB broth supplemented with 100 µM of specified compounds previously dissolved in dimethyl sulfoxide (DMSO; Merck) or with the same volume of DMSO. Simultaneously, *Vibrio harveyi* BB120 was grown in Marine Broth at 30 °C for 16 hrs with shaking. Cultures of *V. harveyi* were collected and 1:5000 dilutions into fresh AB medium were prepared. Then, ninety µl of diluted *V. harveyi* cultures were mixed with ten microliters of sterile-filtered culture media of PAO1 (treated or not with compounds) containing all the QS molecules released by PAO1, including AHL and AI-2 able to stimulate the *V. harveyi* bioluminescence. The mixtures were seeded into a sterile 96-well white

microtiter plate (Costar). Plates were incubated overnight at 30 °C and luminescence was quantified with a MultiPlateReader VictorX2 (Perkin Elmer) (Waters *et al.*, 2006). *V. harveyi* bioluminescence was normalized to bacterial growth (OD 620 nm). PAO1 not exposed to any compound was used as positive control and its bioluminescence (normalized to bacterial growth) was arbitrarily set to 100% of the signal.

2.5 AHL analysis

The analysis of QS molecules released by PAO1 is based on previously published procedures (Ortori *et al.*, 2011; Liu *et al.*, 2019) and adopts LC-MS technology using reverse phase chromatography. PA01 (10^6CFU/mL) was cultured in LB with and without compounds and incubated at 37 °C. Culture supernatants were collected at specified time points (0, 4, 8, 16, 24, 36, and 48 hrs) and sterilized by filtration. An aliquot was used to quantify the AHL. The instrument comprises an Agilent 1260 LC system combined with a Varian 500MS equipped with Electrospray Ion source (ESI). The method worked with nebulizer pressure at 30 psi, drying gas pressure at 15 psi, drying gas temperature at 290°C capillary voltage 80 V, Rf loading 80%. Column was an Eclipse XDB C18 2,1 x 150 mm (3.5 micron). The gradient started with 60% water, 1% formic acid (A), and 60% ACCN, then in 10 minutes went to 4% A and remained isocratic up to 12 minutes (min). Then back to the initial condition at 14 min. The compounds were detected on the basis of their *m/z* value and literature comparison (Ortori *et al.*, 2011; Liu *et al.*, 2019) as C6HSL (*m/z* 200), 3-oxo-C9-HSL (*m/z* 256), *N*-[(3*S*)-2-oxooxolan-3-yl]dodecanamide (m/z 256), 3-oxo-*N*-(2-oxotetrahydro-3-furanyl)dodecanamide (*m/z* 270), 3-oxo-C12-HSL (*m/z* 284), 3-oxo-C12-HSL isomer 1 and 2 (*m/z* 298). Calibration curves were obtained using the reference compound 3-oxo-C12-HSL (Merck) in the concentration range of 0.5-150 µg/mL.

2.6 Growth inhibition assay

Molecules that showed a ≥50% decrease in PAO1-induced bioluminescence in *V. harveyi* BB120 were further evaluated for their potential toxic effect on PAO1. Overnight cultures of PAO1 were collected, centrifuged, and suspended in LB-broth at 10^8 CFU/mL. Bacteria were dispensed in sterile 96-well microtiter plates at a final concentration of $1x10^6$ CFU/100 µL of LB broth/well. PAO1 was cultured with DMSO or in the presence of selected molecules for up to 36 hrs at 37 °C. Bacterial growth was monitored by measuring the optical density at 620 nm at different time points.

2.7 Cytotoxicity assay

To exclude cytotoxic effects on eukaryotic cells, the selected molecules were tested on A549 (CCL-185, ATCC) cell line as a model of the human respiratory tract epithelium. Cells were cultured in DMEM supplemented with 10% FBS and 1% penicillin/streptomycin (all provided by Gibco) and then seeded in 96 well/plates. After 24 hrs, compounds were added to a final concentration ranging from 0 to 10 mM. Following overnight incubation at 37 °C, the culture medium was substituted with fresh one. Following additional 48 hrs of incubation at 37 °C, cells were incubated for 4 hrs at 37°C with MTT solution (5mg/mL, Merck). Formazan crystals were solubilized in 100 µL of SDS 10% w/vol, HCl 0.01 N, and the absorbance was recorded 16 hrs later at 590 nm using a microplate reader (Varioskan Lux Reader, Thermo Fisher Scientific).

2.8 RNA isolation and measurement of gene expression by qRT-PCR

PAO1 was cultured in LB with DMSO or supplemented with the selected molecules for 24 hrs at 37 °C. Then cultures were centrifuged, the medium discarded and total RNA was isolated and purified using the GRS Total RNA Kit – Bacteria (#GK16.0100, GRISP Research Solution) with mechanical

and enzymatic cellular disruption, according to the manufacturer's instructions and as previously described (Bernabè *et al.*, 2021). A treatment with DNase I was used to remove contaminating DNA. The RNA yield and purity were assessed by measuring the ratio of UV absorbance at 260 and 280 nm and only samples in the range of 1.8-2 were used. In preliminary experiments, we observed that expression of most AHL-regulated genes peaked after 24 hrs of culture (SI Figure 1); thus PAO1 cultures were collected after 24 hrs of incubation.

The cDNA was generated using a high-capacity cDNA RT kit with an RNAse inhibitor (Applied Biosystems) using a Bio-Rad thermocycler. Quantitative PCR (qRT-PCR) was conducted to determine the levels of transcripts of interest using specific primers indicated in Table 1. The housekeeping gene *proC* was used. The data were analyzed using the $2^{\Delta\Delta Ct}$ method, PAO1 cultures without treatment were used as reference. The qRT-PCRs were conducted using SYBRR green mixture (iScript One-Step RT-PCR kit with SYBR green, Bio-Rad). Annealing temperature and primer sequences and amplicon sizes are reported in Table 1. Samples were assayed in triplicate.

2.9 Effect of selected molecules on PAO1 biofilm resistance to antibiotic treatment

Selected compounds were tested for their direct or synergistic activity with conventional antibiotics on PAO1 biofilm formation. To better reproduce the growth condition in the lung, we used the Artificial Sputum Medium (ASM) prepared as described by Kirchner (Kirchner *et al.*, 2012). ASM is a culture medium developed to mimic chronic lung colonization by *P. aeruginosa* helpful in evaluating therapeutic procedures and studying antibiotic-resistance mechanisms (Sriramulu *et al.*, 2005). An overnight culture of PAO1 grown in LB at 37 °C was diluted in ASM at 10^8 CFU/mL and 1 mL was seeded into 24 well polystyrene plates and incubated at 37°C with low shaking (75 rpm/min). After 36 hrs of incubation, the bacterial biofilm was disrupted using 100 µl of cellulase (100 mg/ml, Merck, diluted in 0.05 M citrate buffer [9.6 g/l Citrate in water; pH to 4.6 with NaOH]) and incubated at 37 °C with shaking (150 rpm/min) for 1 hr. To determine viable cells released from disrupted biofilms, we added 100 µl of 0.02 % (v/v in distilled water) resazurin to each well. The plates were incubated at 37 °C for 3 hrs with shaking (150 rpm/min). The non-fluorescent resazurin (blue) is reduced to highly fluorescent resorufin (pink) by dehydrogenase enzymes in metabolically active cells. Thus, the amount of resorufin produced is proportional to the number of viable bacteria. The resorufin formed in the assay was quantified by measuring the relative fluorescence with Multi Plate Reader Victor X2 (Perkin Elmer) (Ex=560nm, Em=590nm). In preliminary experiments, we determined that PAO1 biofilm formation in ASM increased for 24 hrs and then plateaued until 40 hrs (SI Figure 2A). Thus, we decided to add treatments (QS inhibitor, 100 µM ± antibiotic, $MBIC_{50}$) after 24 hrs of biofilm incubation (effect on pre-formed biofilm). The amount of viable bacteria in the biofilm was quantified after additional 16 hrs (Kirchner *et al.*, 2012). The Minimum Biofilm Inhibitory Concentration (MBIC) of aztreonam was determined by adding different concentrations of the antibiotic to PAO1 seeded in ASM for 24 hrs and the $MBIC_{50}$ settled at 4 µg/mL (SI Figure 2).

2.10 Virulence factors analysis

Pyocyanin production: the production of pyocyanin was investigated as described by Ugurlu *et al*. (Ugurlu *et al.*, 2016). Overnight cultures of PAO1 or clinical isolates were collected, centrifuged, and resuspended in LB at 10^8 CFU/mL. Then 10^6 CFU were incubated at 37 °C in LB with DMSO or supplemented with selected compounds. After 24 hrs, cultures were centrifuged, clear supernatant was collected, and chloroform was added at a 3:5 (v/v) ratio and mixed by inversion. The separated

chloroform layer containing pyocyanin was transferred into a new collection tube and acidified with 0.2M HCl. This reaction led to a pink solution that was aliquoted into a 96-well microtiter plate and optical density at 520 nm was quantified with a microplate reader (Varioskan Lux Reader, Thermo Fisher Scientific).

Elastase B production: elastolytic activity of PAO1 and clinical isolates was assessed following the method described by Parasuraman *et al.* (Parasuraman *et al.*, 2020). Samples were prepared as described above and cell-free supernatants were added (1:9 v/v ratio) to Elastin Congo Red buffer (ECR buffer: 100mM Tris, 1mM $CaCl_2$, pH 7,5) containing 20 mg of Elastin Congo Red (Merck). The mixtures were incubated at 37 °C for 3 hrs with shaking (150 rpm/min). After incubation, tubes were centrifuged (10000 rpm for 5 min) to remove the insoluble material. One hundred microliters of the supernatants were transferred in a 96 well microplate and optical density at 540 nm was quantified with a microplate reader (Varioskan Lux Reader, Thermo Fisher Scientific).

Swarming motility: *P. aeruginosa* culture samples were prepared as described in pyocyanin quantification. After overnight incubation, 10 µL of the culture previously diluted 1:10 was seeded on Agar plates containing medium formulated with 1% tryptone, 0.5% NaCl, 0.5% agar, and 0.5% filter sterilized di D(+)-Glucose (Merck). The plates were incubated at 37 °C in the upright position for 36 hrs and then photographed. The distance movement was calculated using the freely available software ImageJ. Plates inoculated with not-treated PAO1 were used as the positive control (Bernabè *et al.*, 2021).

Rhamnolipids quantification: rhamnolipids quantification was performed as described before with some modifications (Rasamiravaka *et al.*, 2016). PAO1 cultures, treated with GM-50 or DMSO, were grown under shaking (175 rpm) at 37 °C for 24 hrs in LB-MOPS medium (Difco). At the end of incubation, cultures were centrifuged (3200 x g; 24 °C; 5 min). Ten mL of supernatant were filtered to remove residual cells and pH was adjusted to 2/3 using 1N HCl. Then ethyl acetate was added at a 1:1 (v/v) ratio and vigorously vortexed for 20 sec. The upper phase was evaporated into a new tube in a speed vac centrifugal evaporator. Dry rhamnolipid extracts were then dissolved in 2 mL chloroform and mixed with 200 µL of methylene blue solution (Merck). Tubes were vigorously mixed and after phase separation (15 min) the lower phase (chloroform) was transferred to a new tube and HCL 0.2N was added at a 1:2 (v/v) ratio. Samples were vortexed and left at room temperature for 10 min. Finally, the upper acid phase was transferred to a 96-well microplate and the absorbance was measured at 638 nm.

2.11 Cytokine assays

To assess the ability of PAO1 to induce an inflammatory phenotype in epithelial cells, we evaluated the release of interleukin (IL)-8 and IL-6 in human alveolar epithelial cells A549. PAO1 was cultured in LB medium supplemented with GM-50 at 100µM or equal volume of DMSO. After 24 hrs, bacteria were collected, centrifuged, and added to A549 monolayers at a MOI of 1:20 (eukaryotic cells: bacteria). Bacteria and cells were incubated at 37 °C and 5% CO_2. After 2 hrs, the culture medium was removed, cells were washed with PBS 1X, and monolayers were incubated with DMEM containing 200 µg/mL gentamycin sulfate (Merck) to kill residual bacteria. After 24 hrs of incubation at 37 °C, the supernatants were collected and centrifuged at 13000 rpm for 6 min. Then, clear supernatants were stored in aliquots at -80 °C until cytokine quantification by ELISA. The levels of IL-8 and IL-6 were measured using human IL-8 and IL-6 ELISA kits (ImmunoTools) according to the manufacturer's

protocol and as described elsewhere (Carta *et al*., 2018). Each tested sample was derived from three independent experiments run in triplicate.

2.12 Quantification of associated and internalized bacteria

To determine the effect of selected compounds on PAO1 adhesion to or internalization in epithelial cells, we followed procedures described by Hawdon *et. al* (Hawdon et al., 2010) with some modifications. A549 cells (10^5/well) were seeded on 24 well plates and cultured for 2 days until they reached approximately 90% confluence. PAO1, cultured for 24 hrs in LB medium supplemented with DMSO or GM-50 at 100μM, were collected, centrifuged, and added to A549 monolayers at an MOI of 1:20 (eukaryotic cells: bacteria). Bacteria and cells were incubated for two hrs at 37 °C and 5% CO_2; after that, the culture medium was removed, and cells were washed three times with sterile PBS to remove non-adhering bacteria.

To quantify bacteria associated with epithelial cells, we added 300 μl of 0,05% trypsin-EDTA. Following incubation for 5 min at 37 °C, cells were collected and lysed (5 min at 37 °C) by adding 700 μL of 0.1% Triton X-100. Lysates were properly diluted, seeded into LB agar plates, and incubated at 37 °C for 24 hrs. Bacterial colonies were counted to enumerate bacteria associated with A549 monolayers. The results represented the amount of both internalized and adherent bacteria (CFU/cell).

To specifically enumerate the internalized bacteria, after 2 hrs of infection, monolayers were washed three times with PBS. Then, DMEM supplemented with 10% FBS, 1% penicillin/streptomycin (Gibco), and 200 μg/mL gentamicin sulfate was added to each well to wipe out extracellular bacteria. After 90 min, the culture medium was removed, and cells were washed three times and lysed as described above. After proper dilutions, samples were seeded in LB agar plates and incubated at 37 °C and the colonies enumerated after 24 hrs represent the number of internalized bacteria. All experiments were performed three times with triplicate determinations.

2.13 *In vivo* assays

To investigate the ability of selected compounds to control *P. aeruginosa* infection, we used *Galleria mellonella* larvae, an inexpensive invertebrate model with no ethical constraints. These larvae possess innate immune responses and are ideal for rapid *in vivo* studies (Tsai *et al*., 2016). Larvae (~500mg) were inoculated with 10 CFU of PAO1. Two hrs later, larvae were injected with 100 μM GM-50 or vehicle (PBS + 0.05% DMSO). Compound GM-32 resulting as inactive at the first screening was used as a negative control. Survival was recorded for up to 40 hrs in treated and not-treated invertebrates. All experiments were conducted three times with 30-50 determinations for each condition.

2.14 Computational Methodology

All the computational methodologies were carried out on a 32 Core AMD Ryzen 9 3905X, 3.5 GHz Linux Workstation (O.S. Ubuntu 20.04) equipped with GPU (Nvidia Quadro RTX 4000, 8 GB).

Protein structures. The structure of LasR was retrieved from the Protein Data Bank (PDB-ID: 6d6a, chain A) (O'Reilly *et al.*, 2018), whereas the structures of RhlR, LasI and RhlI were obtained from the AlphaFold Protein Structure Database (IDs: A0A411HE41, P33883, A0A411F6V2, respectively) (Jumper J *et al*., 2021; Varadi M, *et al*. 2022)

Molecular docking simulations. The three-dimensional structures (".mol2" format with explicit hydrogenation at pH=7.2) of the compounds GM-50, C4HSL, and 3-oxo-C12-HSL were prepared with OpenBabel ver. 3.1.1 starting from the SMILES code (O'Boyle *et al.*, 2011) and then converted into the appropriate ".pdbqt" files using AutoDock (AD) ver. 4.2 (Morris *et al.*, 2009). All the protein

structures were aligned to the LasR structure and the appropriate ".pdbqt" files were prepared using AutoDock (AD) ver. 4.2. The following binding complex were simulated: GM-50/LasR, GM-50/RhlR, GM-50/LasI, GM-50/RhlI, 3O-C12-HSL/LasR, C4-HLS/RhlR. All the docking simulations were conducted in a box (centre: x = 57.502, y =15.631, z = 6.591) with grid spacing = 0.375 Å and 40 x 40 x 40 points. The docking poses were generated using the Lemarkian genetic algorithm (Morris *et al.*, 1998) with the following parameters: population size = 250; number of evaluations: 2,500,000; maximum number of generations = 27,000; mutation rate = 0.02; crossover rate = 0.8. For each simulated pair compound/protein, we found that the lowest energy cluster contained the lowest energy pose (that was, in turn, analyzed in-depth to identify the compound/protein interactions) and was also the most populated cluster. The selected binding poses were used as starting structures for molecular dynamics simulations.

Molecular dynamics simulations. All the molecular dynamics simulations were conducted with the Gromacs ver. 2021.1 software (Pronk S *et al*., 2013; Van der Spoel *et al*., 2005), using the CHARMM36 forcefield (Huang J *et al*., 2013) for both the proteins and the ligand. The parameters files required for the ligands were obtained through the CGenFF website (Vanommeslaeghe K *et al*., 2012). The long-range electrostatic interactions were modeled with the PME method. The short-range Coulomb and Van der Waals interactions were subjected to a cut-off of 1.2 nm. The LINCS algorithm was used to constrain the bonds involving hydrogen atoms. Each complex protein/ligand was centered in a cubic box, solvated (water model: TIP3P), and neutralized with Na^+ and Cl^- ions (final concentration: 0.15 M). The structures were then equilibrated in the NVT (200 ps, T=300 °K, v-rescale thermostat, dt=0.001 fs) and the NPT (200 ps, T=300 °K, P=1 bar, Berendsen barostat, dt=0.002 fs) ensembles. Production runs were conducted for 50 ns using the Parrinello-Rahman barostat (Parrinello M *et al*., 1981). The root-mean squared deviations and the interaction energies were obtained through the "gmx rms" and "gmx energy" routines.

2.15 Data management and statistical analysis

Clinical isolates were collected at the Clinical Microbiology Laboratory of Padua University Hospital and identified using randomly generated numerical ID. Data relative to patients were kept in a separate database following applicable laws and guidelines on privacy management. Personal data of patients were not shared among the participants of the study.

All reported experiments were conducted at least three times with triplicate determinations for each condition. Data were analyzed by two-way analysis of variance (ANOVA) followed by Bonferroni multiple comparison post hoc test using GraphPad Prism (version 8.0). A *P*-value of 0.05 or less will be considered statistically significant. Cartoons in Figures 4H, 5E, and 8 were realized using Microsoft PowerPoint® 2010 and Microsoft Paint®.

3. Results

3.1 Bioluminescence assay to identify AHL quorum sensing inhibitor candidates

To screen our library of 81 compounds for interference with the AHL-mediated quorum sensing system of PAO1, we performed a bioluminescence assay using the reporter strain *Vibrio harveyi* BB120, in which bioluminescence emission proportionally increases in response to AHL (SI Figure 1). To identify when AHL reaches its highest level in a PAO1 culture, we collected the PAO1 culture medium at different time points and determined the amount of AHL by adding 10 µL of PAO1 supernatants to

V. harveyi cultures. Sixteen hrs later, we quantified *V. harveyi*-produced luminescence using Varioskan LUX Multimode Microplate Reader. Bioluminescence of *Vibrio harveyi* BB120 exposed to PAO1 culture supernatants was barely detectable up to 6 hrs, significantly increased at 16 hrs, and peaked at 24 hrs of incubation. No further increase was observed at longer incubation times (SI Figure 1). Moreover, liquid chromatography plus mass-spectrometry analysis of PAO1 culture media confirmed that AHL reached the highest level after 24 hrs of incubation (SI Figure 1). Indeed, a direct correlation was observed between AHL levels in the PAO1 culture medium and *V. harveyi*-produced luminescence (SI Figure 1). Therefore, the following tests were carried on by treating PAO1 cultures with the specific synthetic small molecules for 24 hrs and detecting the presence of AHLs using *V. harveyi* BB120. We arbitrarily assigned a 100% luminescence value to the signal produced by *V. harveyi* following incubation with PAO1 + vehicle (DMSO 0.05%). Data relative to the screened 81 compounds are reported in SI Figure 2. Sixty-one molecules were considered ineffective (i.e., they caused an increase in bioluminescence emission or a reduced luminescence emission by less than 20% compared to PAO1 treated with DMSO); twelve molecules reduced the bioluminescence emission only by 21-49% and were abandoned since considered weakly active. Nine molecules reduced AHL-mediated bioluminescence in *V. harveyi* BB120 by more than 50% (Supplementary Table 1). The nine molecules showing significant inhibitory activity were subjected to a second screening assay, evaluating their effect on the transcription levels of AHL-regulated genes by molecular analysis. JAF548-related luminescence did not increase after the addition of PAO1 supernatant (data not shown).

3.2 Inhibition of transcription of *las*- and *rhl*- regulated genes in the presence of selected compounds

Since the antivirulence activity of AHL-QS inhibitors correlates with the reduced expression of las- and rhl-regulated genes, we determined the ability of the selected 9 phenolic derivatives to interfere with AHL-induced expression of specific genes. Thus, using qRT-PCR we quantified the mRNA transcripts of lasI and rhlI (genes involved in the synthesis of AHLs), lasR and rhlR (genes coding for AHLs receptors), and lasB and rhlA (genes coding for elastase B and rhamnolipids, respectively) in PAO1 cultured for 24 hrs in the presence of the selected small molecules. Molecular analysis revealed that 2 out of 8 compounds (GM-22 and GM-79; Figure 1A and B) stimulated the expression of AHL-dependent QS signaling systems. GM-50 showed the highest inhibitory activity (Figure 1 A and C). GM-50 was the most potent compound in reducing the expression of rhlR/I/A and lasB and we observed a moderate effect on LasR/I (Figure 1A and B). Afterward, we performed a dose-response experiment to identify the lowest effective dose. We found that GM-50 is active on the Las pathway only at 100 µM, whereas it maintains the inhibitory activity on the Rhl pathway also at 10 µM (Figure 1C).

3.3 Compound GM50 does not interfere with bacteria viability and is not toxic in eukaryotic cells

To exclude that GM-50 reduced AHL production because of direct toxicity on bacteria we cultured PAO1 for 24 hrs in 96 well in the presence of DMSO 0.05% (vehicle) or 100 µM of GM-50. We monitored optical density to measure the microbial growth curve for 36 hrs. As reported in Figure 2A, GM-50 had no significant effects on bacterial growth at the tested concentration. Moreover, the colony count assay was not affected by GM-50 (Figure 2B).

To investigate GM-50 toxicity, we exposed A549 human lung carcinoma epithelial cell line to the compound at concentrations ranging from 0 to 10 mM for 24 hrs. Cell viability was measured by MTT

assay. GM-50 showed minimal cytotoxic activity at concentrations higher than 200 µM, greater than the one effective on AHL-dependent QS signaling systems (Figure 2C). Overall, GM-50 showed no direct toxicity on prokaryotic and eukaryotic cells.

3.4 GM-50 inhibits AHL production

The LC-MS measurements allowed us to observe that the treatment with compounds GM-50 inhibits AHL production (Figure 3). As evidenced in the representative chromatograms in Figure 3A, cultures of PAO1 treated with GM-50 showed a reduction in the intensity of the peaks ascribable to the produced AHLs (Figure 3B). This result correlates with the bioluminescence assay results (Figure 3C) and with the ability of the compound to inhibit the AHL-regulated genes (Figure 1C).

3.5 Compound GM-50 strongly reduces the production of virulence factors regulated by AHL-signalling and its gene expression

AHL-dependent QS signaling systems modulate the expression of a large group of genes regulating virulence in *P. aeruginosa*, such as biofilm formation, swarming motility, pyocyanin synthesis, and elastase B and rhamnolipids production. To verify whether GM-50 inhibited elastase B, pyocyanin, and rhamnolipids production, we compared the production of these toxins in vehicle-treated PAO1 cultures to PAO1 cultures exposed to the compound. After 24 hrs of incubation, GM-50 significantly reduced the production of virulence factors in PAO1: it was active in reducing pyocyanin (approximately by 70%), rhamnolipid production (by 40%), and elastase B release (by 20%) (Figure 4 A, C, and D). Notably, GM-50 inhibited the expression of *rhlA* and *phzA*, genes under the QS control and involved in rhamnolipids and pyocyanin synthesis (Figure 4 B and E). To evaluate the ability of the compound to perturb swarming motility, PAO1 cultures were first cultured for 24 hrs in the presence or absence of the compound. They were then seeded in the centre of the agar plates to evaluate bacterial movements. As shown in Figure 4F, GM-50 reduced by 20% PAO1 swarming.

3.6 GM-50 potentiates Aztreonam activity in mature PAO1 biofilm

To evaluate the impact of GM-50 on biofilm disruption, we treated PAO1 mature biofilm (24 hrs of growth with slow agitation). Since previous studies reported that disrupting QS signaling might enhance sensitivity to traditional antibiotics, we decided to test the compounds in combination with Aztreonam, an antibiotic recommended in treating chronic *P. aeruginosa* infections (Brackman *et al.*, 2011). PAO1 incubated with the medium containing DMSO 0.05% was used as a negative control and assigned 100% biofilm formation. We previously identified at 4µg/mL the aztreonam $MBIC_{50}$ (SI Figure 3). Compared to the negative control, Aztreonam alone reduced biofilm by 40% (Abx, Figure 4G). GM-50 (100 µM) was ineffective on pre-formed biofilm when used alone (Figure 4G). However, the combination of GM-50 with aztreonam at $MBIC_{50}$ (see the experimental design in Figure 4H) reduced by 60% the mature biofilm. Thus, the addition of compound GM-50 significantly enhanced aztreonam activity on biofilm disruption.

3.7 Compound GM-50 reduces PAO1-mediated epithelial cell activation

Pulmonary infections caused by *P. aeruginosa* are commonly associated with the activation of intracellular signals resulting in the release of cytokines and chemokines. In particular, IL-8 plays a crucial role in recruiting inflammatory cells enhancing neutrophil-mediated lung injury (Sar *et al.*, 1999). A549 cells infected with PAO1 at a MOI of 1:20 released significant amounts of IL-8 and IL-6 (Figure 5A and B). Incubation with GM-50 significantly reduced PAO1-induced IL-8 and IL-6 secretion (Figure 5A and B).

Bacterial adhesion to airway epithelial cells and internalization are critical steps to colonize and damage the airway mucosa. In *P. aeruginosa*, they are both regulated by QS signaling (Strateva *et al*., 2011). Therefore, we evaluated the effect of the phenolic derivative GM-50 on PAO1 adhesion and internalization in A549. As reported in Figure 5 C and D, GM-50 reduced *P. aeruginosa* adhesion by almost 50% and reduced the internalization of PAO1 in airway epithelial cells by 45%.

3.8 Compound GM-50 decreases PAO1-induced mortality in *G. mellonella* larvae

We evaluated the *in vivo* effect of treatment with GM-50 in the *G. mellonella* model system (see the experimental design in Figure 5E). The QS inhibitor was not toxic for *G. mellonella* at the concentrations used (data not shown). Following injection of 10 CFU of PAO1, a significant decrease in survival of *G. mellonella* at 40 hrs was observed, and mean survival time was reported at 27 hrs compared to PBS injected larvae (Figure 5F and G). Conversely, ~75% of *G. mellonella* larvae challenged with PAO1 and treated with GM-50 survived 36 hrs after infection. On the contrary, treatment with the negative control GM-32, a molecule devoid of activity on AHL-dependent QS signaling (SI Figure 2), had no significant effect on PAO1-induced *G. mellonella* larvae mortality and mean survival time (Figure 5G). Overall, our results demonstrate that GM-50 was able to protect *G. mellonella* larvae from *P. aeruginosa* PAO1 infection.

3.9 GM-50 inhibits the production of virulence factors in clinical isolates

Since laboratory strain PAO1 significantly differs from field strains, we collected 20 *P. aeruginosa* isolates from the sputum of patients with respiratory tract infections. We assessed the anti-virulence activity of GM-50 on these clinical isolates. For each isolate, the values of the virulence factors obtained by incubating the strain in LB containing only DMSO 0.05% were set as the 100% of the activity. As expected, the compound GM-50 was not active on all strains probably due to genetic modifications acquired by clinical isolates. However, as reported in Figure 6, GM-50 significantly reduced elastase and pyocyanin production in almost all isolates. Remarkably, GM-50 is strongly active in pyocyanin inhibition, a virulence factor mainly regulated by rhl-QS pathway (Dekimpe *et al*., 2009). Moreover, these results are in accordance with qRT-PCR pointing out the rhl-pathway as the GM-50 target.

3.10 GM-50 docking and molecular dynamics simulations

To dissect the mechanisms of action of GM-50 on multiple QS systems of *P. aeruginosa*, we performed molecular docking simulations focusing on RhlR, RhlI, LasR and LasI, four proteins involved in the two QS pathways regulating the production of the virulence factors described above. While in the case of LasR different three-dimensional structures were present in the Protein Data Bank repository, the structures of RhlR, LasI, and RhlI were derived from the AlphaFold repository. AlphaFold is a well-recognized recently developed artificial intelligence program that is able to predict the 3D structures of (potentially) any protein (Jumper J *et al*. 2021; Varaldi M *et al*., 2022). For comparison purposes, C4HSL and 3-oxo-C12-HSL, the physiological activator of RhlR and LasR respectively were also docked in the receptor. The two AHLs were not docked in LasI and RhlI since it is conceivable that both C4HSL and 3-oxo-C12-HSL are readily released from the synthases upon production.

The predicted complexes were then submitted to molecular dynamics (MDs) simulations, to verify the stability (and thus the reliability) of the docked structures. The complexes GM-50/LasR, GM-50/RhlI, and GM-50/LasI resulted unstable; the compound was readily released from the predicted binding sites

and the simulations were stopped after 10 ns (Figure 7 A, B, and C, respectively), suggesting that these proteins are not targeted by the compound.

Conversely, the complex GM-50/RhlR (Figure 8A) was stable for the entire simulation (50 ns; Figure 8 B and C), confirming RhlR as the most probable biomolecular target. The interaction energy between GM-50 and RhlR (computed as the sum of the average short-range Coulombic and the short-range Lennard-Jones interaction energies between ligand and protein), measured throughout the simulation, remained very stable (-45.23 ± 3.00 Kcal/mol; Figure 8D). For comparison purposes, the interaction energy between C4HSL and RhlR was measured, yielding a value of -54.83 ± 2.92 Kcal/mol (Figure 8D).

4 Discussion

Pseudomonas aeruginosa is an opportunistic pathogen able to cause infections, particularly in patients with chronic wounds, chronic respiratory tract diseases, urinary bladder catheters, or patients admitted to intensive care units (Vincent *et al*., 1995). The unique ability to establish persistent infections is often associated with the selection of multiple antibiotic-resistance strains. This observation strengthens the need for new drugs and therapeutic approaches to treat PA infections. QS signaling tightly regulates *P. aeruginosa* biofilm formation and virulence and plays a prominent role in establishing and maintaining chronic infections, thus representing a reasonable therapeutic target. Indeed, infections caused by *P. aeruginosa* whose QS communication systems have been disabled by mutation(s) are more readily cleared by the host organism than their wild-type counterparts (Bjarnsholt *et al.*, 2005; Bjarnsholt *et al.*, 2013). Moreover, molecules affecting the QS signaling system of *P. aeruginosa* promote infection clearing in different experimental models (Dong *et al*., 2007; Luo *et al.*, 2017; Proctor *et al.*, 2020). Although these compounds *per se* cannot eradicate bacterial infections they blunt pathogen aggressiveness by reducing microbial virulence, thus decreasing the severity of tissue damage and increasing the success of host immune defence and traditional antibiotic treatments (Soukarieh *et al.*, 2018). Granting the rationale of QS inhibitors in *P. aeruginosa*, the identification of effective molecules has to face several drawbacks, including the complexity and the lack of structural data on critical elements of QS signaling in this pathogen.

Acyl-homoserine lactones (AHL)-dependent QS circuits, the Las and Rhl QS systems (Pearson *et al.*, 1994), regulate the production of a variety of virulence factors and suppress the response of the host immune system. For these reasons, they have been targeted in several studies (Hossain *et al.*, 2017; Ahmed *et al.*, 2019; Piepenbrink *et al.*, 2020). Thus, natural derivatives from plants, fungi, and marine organisms and synthetic molecules were tested as QS inhibitors (Kalia *et al*., 2013), even against *P. aeruginosa* (Yin *et al.*, 2015; Chen *et al*., 2017). The mechanisms involved in QS inhibition by natural polyphenols are mainly based on antioxidant and antimetabolic effects whereas molecular docking analysis reported high binding affinity to the LasR domain mainly because of the electrostatic interactions of the natural compounds with the protein (Zhu *et al*., 1998; Teplitski *et al*., 2004; Ni *et al.*, 2008; Chen *et al*., 2017). Moreover, natural polyphenols are extremely unstable molecules (Deng *et al*., 2018) and no one has yet been available for treatment. It has been reported that natural phenolic compounds from plants, such as eugenol, tea polyphenols, and thymol, possess a QS inhibitory activity preventing the production of virulence-associated factors and biofilm formation in *P. aeruginosa* (Ugurlu *et al.*, 2016; Yang *et al.*, 2021; Antunes *et al.*, 2021; Walsh *et al.*, 2019). Therefore, to identify

active non-toxic molecules endowed with inhibitory activity on AHL-dependent QS signaling, we have screened a library of 81 phenolic derivatives generated in our laboratories. Through a two-step screening, namely AHL biosensors and quantitative RT-PCR, we identified a compound showing significant inhibitory effects on AHL-dependent QS-regulated genes *lasI/R, rhlI/R* and their mediated virulence factors *lasB* and *rhlA*. Analysis of the AHL profile by LC-MS confirmed the reduced release of the signal molecules in PAO1 exposed to GM-50 (Figure 3).

The assessment of the AHL activity showed that the anti-QS activity of the phenolic derivative may likely stem from the binding between the selected molecules and the receptor protein (Wagner *et al.*, 2006). By combining *in silico* docking and molecular dynamics experiments, we demonstrated that GM-50 steadily binds Rhl receptor, while it is not able to stably bind other potential targets such as LasR, LasI, or RhlI. As previously reported, $^{60}Trp_{LasR}$ is a key residue for either the positive or negative modulation of LasR activity (Gerdt *et al.*, 2014). It is plausible that the analog residue ^{68}Trp in RhlR may play the same regulatory role. Indeed, GM-50 established a lasting and strong H-bond with ^{68}Trp through one of the phenolic functions. Other interactions that were predicted between GM-50 and the target protein are one H-bond between the ^{81}Asp sidechain and the other phenolic function of GM-50, as well as a π-π stacking with ^{72}Tyr sidechain. The binding mode remained stable for the entire 50 ns of simulations. For comparison, we also run in parallel the MDs simulation of the complex C4HSL/RhlR. The binding between the physiological ligand and the protein involved the interaction with ^{68}Trp, further confirming the importance of this residue in RhlR activity regulation (Figures 7 and 8). The comparison between the short-range (both Coulombic and Lennard-Jones) protein/ligand interaction energies suggests that GM-50 ($E_{interaction}$ ~ -45 Kcal/mol) can bind the target protein in the presence of the activator ($E_{interaction}$ ~ -55 Kcal/mol) but relative high concentrations of the phenolic inhibitor are required, suggesting that GM-50 still deserves structural improvement. For the sake of clarity, at this stage we have not computed the binding free energies (ΔG) but only the molecular mechanics interaction energies throughout the MDs simulations. Due to these observations, we predict that GM-50 preferentially binds RhlR, accordingly with the significant activity in reducing genes involved in the *rhl* pathway (Figure 1). Recent reports evidence the importance of rhl role in virulence, demonstrating that LasR-mutants frequently occur among clinical isolates. More than half of LasR-mutants isolates retain a LasR-independent RhlR activity (Groleau *et al.*, 2021).

Inhibition of AHL-dependent QS signaling exerts favorable effects since down-regulating expression of several virulence factors such as pyocyanin, elastase B, and rhamnolipids will decrease the severity of tissue damage and increase the success of host immune defense (Turkina *et al*., 2019). Two QS pathways control the production of pyocyanin in *P. aeruginosa*. Pyocyanin is a blue-green phenazine pigment able to interfere with the host cellular respiration, chelated iron absorption (Chang *et al.*, 2014), and bacterial competitors (Castañeda-Tamez *et al.*, 2018; Diggle *et al.*, 2003). Elastase B is one of the major proteases produced by *P. aeruginosa*; it is directly involved in tissue damage and prejudicing immune responses ((Husain *et al.*, 2017). Rhamnolipids play a key role in biofilms formation and immune evasion, causing the killing of polymorphonuclear leukocytes and disrupting the mucosal epithelial barrier (Castañeda-Tamez *et al.*, 2018). Our findings indicate that GM-50 is an active phenolic derivative in inhibiting pyocyanin, elastase B, and swarming motility accordingly to the dominant effect on the rhl-gene pathway of this molecule (Figures 1 and 4). Indeed, GM-50 tested at 10 μM still reduced AHL-dependent gene expression, supporting the potential of this compound as

an antivirulence agent in *P. aeruginosa* to counteract AHL-mediated QS systems (Figure 1C). Additionally, *P. aeruginosa*–secreted products may also affect epithelial cell phenotype impairing wound healing, directional migration (Ruffin *et al.*, 2016), and production of inflammatory cytokines through activation of transcriptional factor kappa-B (NF-κB). The inhibition of QS with GM-50 significantly reduced the proinflammatory responses triggered by PAO1 on respiratory epithelial cells and potentially decreased tissue damage (Figure 5).

A strategic pathogenic mechanism for *P. aeruginosa* is the QS-regulated biofilm formation (Ciofu *et al.*, 2015; Azam *et al*., 2019), which makes the eradication of the infection quite challenging and causes chronic inflammation in the underlying mucosa favoring antibiotic resistance (Chua *et al.*, 2016). Thus, the weakening of biofilm by QS inhibitors facilitates antibiotic activity and is viewed as an attractive therapeutic strategy to improve the outcome of *P. aeruginos*a infections. In the present investigation, the biofilms were allowed to develop in Artificial Sputum Medium, a culture medium that mimics the components observed in chronic infections (Kirchner *et al.*, 2012). Compared with control, phenolic derivative GM-50 did not result in direct biofilm inhibition in PAO1. However, we observed that in biofilm GM-50 possessed a synergistic effect with aztreonam, an antibiotic that we selected for its clinical relevance in the treatment of patients with chronic PA infections. Notably, the synergistic effects of GM-50 and aztreonam were observed on mature biofilm, the leading cause of nosocomial and chronic infection (Figure 4). Our results are in agreement with previous reports showing that QS inhibitors such as curcumin, itaconimides, and cinnamaldehyde enhance the activity of antibiotics such as ceftazidime, tobramycin, and colistin, respectively, on biofilm inhibition (Roudashti *et al.*, 2017; Fong *et al.*, 2019; Topa *et al.*, 2020) but are poorly effective by themselves. Overall, the data available offer promising applications of QS inhibitors in combination with antibiotics to control biofilm-associated infections.

The *in vitro* results raise the question of what kind of effect our phenolic derivative might have on *P. aeruginosa* PAO1 virulence *in vivo*. Previous research showed that QS inhibitors block the virulence in *P. aeruginosa* in invertebrate model hosts, protecting *C. elegans*, *D. melanogaster*, or *G. mellonella* larvae (O'Loughlin *et al.*, 2013; Papaioannou *et al*., 2013), and results correlate with mammalian acute infection models (Roudashti *et al.*, 2017). In the insect models, *P. aeruginosa* accumulates and produces QS-dependent virulence factors, such as pyocyanin and elastase B, which are lethal. Compared with that in the untreated PAO1 group, in the *G. mellonella* model, our phenolic derivative GM-50 results in significant therapeutic potential (Figure 5). In a previous study, QS inhibitors such as hypertonic glucose and clofoctol were tested in *G. mellonella* larvae. The first one was injected at 200mg/mL, a concentration higher than the concentration used for GM-50 in the present study (100µM). Clofoctol was used at 100µM, but it affects another PA QS-system, the Pqs, regulated by quinolones (D'Angelo *et al.*, 2018; Chen *et al.*, 2020). Since GM-50 did not alter bacterial growth rates or exert direct antimicrobial activity, our results suggest that inhibiting AHL-dependent Rhl circuits decreases pyocyanin, elastase B, rhamnolipids, and swarming motility. Moreover, GM-50 significantly affected the virulence of the bacteria and the host immune system and prolonged larval survival.

Finally, we tested the compound against PA clinical strains isolated from the respiratory tract of patients since it is well known that PAO1, a strain domesticated by extensive use in the laboratory, might produce results far from *in vivo* conditions for different virulence-related phenotypes (El-Shaer *et al.*, 2016). In accordance with the genetic diversity and phenotypic heterogeneity of *P. aeruginosa*

field strains (Finnan *et al.*, 2004; Nassar *et al.*, 2022; Lebreton *et al.*, 2021), our clinical isolates significantly differed as regard pyocyanin production and swarming motility (data not shown). Although the clinical strains responded differently to treatment, overall, we reported a significant reduction in the production of pyocyanin, swarming and elastase B in most strains tested (Figure 6). The variable efficacy of QS inhibitor molecules on clinical strains is in agreement with previous studies investigating the ability of novel compounds to reduce virulence factors in clinical rather than in reference laboratory strains (García-Contreras *et al.*, 2013; Guendouze *et al.*, 2017). Indeed, clinical strains isolated from patients with chronic infections possibly accumulate mutations in the QS genes (Ciofu *et al.*, 2010). The number of strains and virulence-related phenotypes that we considered in this study are not sufficient to drive a definitive conclusion. However, the strain-dependent response to the phenolic derivative is an issue that deserves to be taken into consideration when testing the anti-virulence properties of QS inhibitors, suggesting that therapeutic application of these molecules requires prior evaluation of activity on the isolate, likely for "traditional" antibiotics and in view of a personalized therapy.

In conclusion, the phenolic derivative GM-50, the most effective compound identified in this study, prevents AHL-dependent Rhl QS signaling and expression of virulence factors and enhances the anti-biofilm activity of aztreonam (Figure 9); it protects *Galleria mellonella* larvae and human A549 lung epithelial cells from *P. aeruginosa* induced killing and inflammatory damage. Molecular docking indicates that GM-50 interacts with RhlR, supporting the potential role for small-molecule modulators of quorum sensing as therapeutics. Moreover, since evidence for LasR-mutants in chronic infections points out the importance of the role of RhlR in infections, we expect that GM-50 represents a fascinating starting point to identify and develop a brand of new chemical classes of QS inhibitors active against *P. aeruginosa*.

5 Conflict of Interest

The authors declare that the research was conducted in the absence of any commercial or financial relationships that could be construed as a potential conflict of interest.

6 Author Contributions

GB, PB, IC designed the experiments, interpreted the data, and wrote the paper; AO and AC revised the Manuscript; GB, MB, AP, MS ran most of the experiments; GM performed the modelling analysis, GDP isolated and characterized clinical isolates; SS and SDA performed and interpreted the HPLC analysis.

7 Funding

Italian Ministry of Education, Universities and Research Grants to IC, and PB. The Italian Cystic Fibrosis Research Foundation (FFC) n. FFC#11/2020 to PB. Cariparo Excellence Project "Restoring Antibiotic sensitivity in Bacteria: a synthetic biology approach (ReActing)" n. 59576. The funding agencies had no role in study design, data collection, interpretation, or the decision to submit the manuscript for publication.

8 Reference

Ahmed, S. A. K. S. *et al.* (2019) 'Natural quorum sensing inhibitors effectively downregulate gene expression of Pseudomonas aeruginosa virulence factors'. Applied Microbiology and Biotechnology, pp. 3521–3535.

Antunes, J. C. *et al.* (2021) 'Eugenol-containing essential oils loaded onto chitosan/polyvinyl alcohol blended films and their ability to eradicate staphylococcus aureus or pseudomonas aeruginosa from infected microenvironments', *Pharmaceutics*, 13(2), pp. 1–22. doi: 10.3390/pharmaceutics13020195.

Azam, M. W. and Khan, A. U. (2019) 'Updates on the pathogenicity status of Pseudomonas aeruginosa', *Drug Discovery Today*. Elsevier Ltd, 24(1), pp. 350–359. doi: 10.1016/j.drudis.2018.07.003.

Bellino, S. F. 'Paolo' D. S. I. M. M. A. P. and Pezzotti (2018) 'Ar-Iss AR-ISS Sorveglianza nazionale dell'Antibiotico-Resistenza 2018'.

Berbabè, G. *et al.* (2021) 'A Novel Aza-Derivative Inhibits agr Quorum Sensing Signaling and Synergizes Methicillin-Resistant Staphylococcus aureus to Clindamycin', *Front Microbiol*, 12, pp. 610859. doi: 10.3389/fmicb.2021.610859.

Bjarnsholt, T. *et al.* (2005) 'Pseudomonas aeruginosa tolerance to tobramycin, hydrogen peroxide and polymorphonuclear leukocytes is quorum-sensing dependent', *Microbiology*, 151(2), pp. 373–383. doi: 10.1099/mic.0.27463-0.

Bjarnsholt, T. *et al.* (2013) 'The in vivo biofilm', *Trends in Microbiology*, 21(9), pp. 466–474. doi: 10.1016/j.tim.2013.06.002.

Borgatti, M, *et al.* (2011) 'Development of a novel furocoumarin derivative inhibiting NF-κB dependent biological functions: design, synthesis and biological effects', *Eur J Med Chem*, 46(10), pp. 4870-7. doi: 10.1016/j.ejmech.2011.07.032.

Boucher, H. W. *et al.* (2009) 'Bad bugs, no drugs: No ESKAPE! An update from the Infectious Diseases Society of America', *Clinical Infectious Diseases*, 48(1), pp. 1–12. doi: 10.1086/595011.

Brackman, G. *et al.* (2011) 'Quorum sensing inhibitors increase the susceptibility of bacterial biofilms to antibiotics in vitro and in vivo', *Antimicrobial Agents and Chemotherapy*, 55(6), pp. 2655–2661. doi: 10.1128/AAC.00045-11.

Carta, D. *et al.* (2018) 'Synthesis and preliminary anti-inflammatory and anti-bacterial evaluation of some diflunisal aza-analogs', *Medchemcomm*, 9(6), pp. 1017-1032. doi: 10.1039/c8md00139a.

Castañeda-Tamez, P. *et al.* (2018) 'Pyocyanin restricts social cheating in Pseudomonas aeruginosa', *Frontiers in Microbiology*, 9(JUN), pp. 1–10. doi: 10.3389/fmicb.2018.01348.

Chang, C. Y. *et al.* (2014) 'Non-antibiotic quorum sensing inhibitors acting against N-acyl homoserine lactone synthase as druggable target', *Scientific Reports*, 4, pp. 1–8. doi: 10.1038/srep07245.

Chen, T. *et al.* (2017) '^{1}H NMR-Based Global Metabolic Studies of Pseudomonas aeruginosa upon Exposure of the Quorum Sensing Inhibitor Resveratrol', J *Proteome Res*, 16(2), pp. 824-830. doi: 10.1021/acs.jproteome.6b00800.

Chen, T. *et al.* (2020) 'Hypertonic glucose inhibits growth and attenuates virulence factors of multidrug-resistant Pseudomonas aeruginosa', *BMC Microbiology*, 20(1), pp. 1–10. doi: 10.1186/s12866-020-01889-2.

Chilin, A *et al.* (2008) 'Coumarin as attractive casein kinase 2 (CK2) inhibitor scaffold: an integrate approach to elucidate the putative binding motif and explain structure-activity relationships', J Med Chem, 51(4), pp. 752-9. doi: 10.1021/jm070909t.

Chua, S. L. *et al.* (2016) 'Selective labelling and eradication of antibiotic-Tolerant bacterial populations in Pseudomonas aeruginosa biofilms', *Nature Communications*. Nature Publishing Group, 7, pp. 1–11. doi: 10.1038/ncomms10750.

Ciofu, O. *et al.* (2010) 'Genetic adaptation of pseudomonas aeruginosa during chronic lung infection of patients with cystic fibrosis: Strong and weak mutators with heterogeneous genetic backgrounds

emerge in mucA and/or lasR mutants', *Microbiology*, 156(4), pp. 1108–1119. doi: 10.1099/mic.0.033993-0.
Ciofu, O. *et al.* (2015) 'Antimicrobial resistance, respiratory tract infections and role of biofilms in lung infections in cystic fibrosis patients', *Advanced Drug Delivery Reviews*. Elsevier B.V., 85, pp. 7–23. doi: 10.1016/j.addr.2014.11.017.
Crousilles, A. *et al.* (2015) 'Which microbial factors really are important in Pseudomonas aeruginosa infections?', *Future Microbiology*, 10(11), pp. 1825–1836. doi: 10.2217/fmb.15.100.
D'Angelo, F. *et al.* (2018) 'Identification of FDA-Approved Drugs as Antivirulence Agents', *Antimicrobial Agents and Chemotherapy*, pp. 1–20. Available at: https://www.ncbi.nlm.nih.gov/pmc/articles/PMC6201120/pdf/e01296-18.pdf.
Dekimpe, V. and Déziel, E. (2009) 'Revisiting the quorum-sensing hierarchy in Pseudomonas aeruginosa: The transcriptional regulator RhlR regulates LasR-specific factors', *Microbiology*, 155(3), pp. 712–723. doi: 10.1099/mic.0.022764-0.
Deng, J. *et al*. (2018) in 'Technological aspects and stability of polyphenols', *Polyphenols: Properties, Recovery, and Applications*, pp 295-323. doi:10.1016/B978-0-12-813572-3.00009-9
Diggle, S. P. *et al.* (2003) 'The Pseudomonas aeruginosa quinolone signal molecule overcomes the cell density-dependency of the quorum sensing hierarchy, regulates rhl-dependent genes at the onset of stationary phase and can be produced in the absence of LasR', *Molecular Microbiology*, 50(1), pp. 29–43. doi: 10.1046/j.1365-2958.2003.03672.x.
Dong, Y. H., Wang, L. H. and Zhang, L. H. (2007) 'Quorum-quenching microbial infections: Mechanisms and implications', *Philosophical Transactions of the Royal Society B: Biological Sciences*, 362(1483), pp. 1201–1211. doi: 10.1098/rstb.2007.2045.
EARS-net (2020) 'Antimicrobial resistance in the EU/EEA (EARS-Net), Annual Epidemiological Report for 2019', *surveillance report*. doi: 10.1177/004947550003000225.
El-Shaer, S. *et al.* (2016) 'Control of quorum sensing and virulence factors of Pseudomonas aeruginosa using phenylalanine arginyl β-naphthylamide', *Journal of Medical Microbiology*, 65(10), pp. 1194–1204. doi: 10.1099/jmm.0.000327.
Finnan, S. *et al.* (2004) 'Genome diversity of Pseudomonas aeruginosa isolates from cystic fibrosis patients and the hospital environment', *Journal of Clinical Microbiology*, 42(12), pp. 5783–5792. doi: 10.1128/JCM.42.12.5783-5792.2004.
Fong, J. *et al.* (2019) 'Itaconimides as novel quorum sensing inhibitors of Pseudomonas aeruginosa', *Frontiers in Cellular and Infection Microbiology*, 9(JAN), pp. 1–11. doi: 10.3389/fcimb.2018.00443.
Freeman, J. A. and Bassler, B. L. (1999) 'A genetic analysis of the function of LuxO, a two-component response regulator involved in quorum sensing in Vibrio harveyi', *Molecular Microbiology*, 31(2), pp. 665–677. doi: 10.1046/j.1365-2958.1999.01208.x.
García-Contreras, R. *et al.* (2013) 'Resistance to the quorum-quenching compounds brominated furanone C-30 and 5-fluorouracil in Pseudomonas aeruginosa clinical isolates', *Pathogens and Disease*, 68(1), pp. 8–11. doi: 10.1111/2049-632X.12039.
Gerdt, J. P. *et al.* (2014) 'Mutational analysis of the quorum-sensing receptor LasR reveals interactions that govern activation and inhibition by nonlactone ligands', *Chemistry and Biology*. Elsevier Ltd, 21(10), pp. 1361–1369. doi: 10.1016/j.chembiol.2014.08.008.
Girard, G. and Bloemberg, G. V. (2008) 'Central role of quorum sensing in regulating the production of pathogenicity factors in Pseudomonas aeruginosa', *Future Microbiology*, 3(1), pp. 97–106. doi: 10.2217/17460913.3.1.97.
Greenberg E. P., Hastings J. W., and U. S. (1979) 'Induction of Luciferase Synthesis in Beneckea harveyi by Other Marine Bacteria', 91, pp. 87–91.
Groleau, M. C. *et al.* (2021) 'Pseudomonas aeruginosa isolates defective in function of the LasR quorum sensing regulator are frequent in diverse environmental niches', *Environmental Microbiology*, 00, pp. 1–14. doi: 10.1111/1462-2920.15745.

Guendouze, A. *et al.* (2017) 'Effect of quorum quenching lactonase in clinical isolates of pseudomonas aeruginosa and comparison with quorum sensing inhibitors', *Frontiers in Microbiology*, 8(FEB), pp. 1–10. doi: 10.3389/fmicb.2017.00227.

Guiotto, A. *et al.* (1984) '6-Methylangelicins: a new series of potential photochemotherapeutic agents for the treatment of psoriasis', *J Med Chem*, 27(8), pp. 959-67. doi: 10.1021/jm00374a005.

Hawdon, N. A. *et al.* (2010) 'Cellular responses of A549 alveolar epithelial cells to serially collected Pseudomonas aeruginosa from cystic fibrosis patients at different stages of pulmonary infection', *FEMS Immunology and Medical Microbiology*, 59(2), pp. 207–220. doi: 10.1111/j.1574-695X.2010.00693.x.

Henke, J. M. and Bassler, B. L. (2004) 'Three parallel quorum-sensing systems regulate gene expression in Vibrio harveyi', *Journal of Bacteriology*, 186(20), pp. 6902–6914. doi: 10.1128/JB.186.20.6902-6914.2004.

Hill, D. *et al.* (2006) 'Antibiotic Susceptibilities of Pseudomonas aeruginosa Isolates Derived from Patients with Cystic Fibrosis under Aerobic , Anaerobic , and Biofilm Conditions', 43(10), pp. 5085–5090. doi: 10.1128/JCM.43.10.5085.

Hossain, M. A. *et al.* (2017) 'Impact of phenolic compounds in the acyl homoserine lactone-mediated quorum sensing regulatory pathways', *Scientific Reports*, 7(1), pp. 1–16. doi: 10.1038/s41598-017-10997-5.

Huang, J. *et al.* (2013) 'CHARMM36 all-atom additive protein force field: validation based on comparison to NMR data', *J Comput Chem*, 34(25), pp. 2135-45. doi: 10.1002/jcc.23354.

Husain, F. M. *et al.* (2017) 'Leaf extracts of Mangifera indica L. inhibit quorum sensing - Regulated production of virulence factors and biofilm in test bacteria', *Frontiers in Microbiology*, 8(APR), pp. 1–12. doi: 10.3389/fmicb.2017.00727.

Jumper, J. *et al.* (2021) 'Highly accurate protein structure prediction with AlphaFold', *Nature*, 596(7873), pp. 583-589. doi: 10.1038/s41586-021-03819-2.

Kalia, V. C. (2013) 'Quorum sensing inhibitors: An overview', *Biotechnology Advances*. Elsevier B.V., 31(2), pp. 224–245. doi: 10.1016/j.biotechadv.2012.10.004.

Kalia, V. C. *et al.* (2019) 'Quorum sensing inhibitors as antipathogens: biotechnological applications', *Biotechnology Advances*. Elsevier Inc, 37(1), pp. 68–90. doi: 10.1016/j.biotechadv.2018.11.006.

Kirchner, S. *et al.* (2012) 'Use of artificial sputum medium to test antibiotic efficacy against Pseudomonas aeruginosa in conditions more relevant to the cystic fibrosis lung', *Journal of Visualized Experiments*, (64), pp. 1–8. doi: 10.3791/3857.

Langendonk, R. F., Neill, D. R. and Fothergill, J. L. (2021) 'The Building Blocks of Antimicrobial Resistance in Pseudomonas aeruginosa : Implications for Current Resistance-Breaking Therapies', 11(April), pp. 1–22. doi: 10.3389/fcimb.2021.665759.

Lansbury, L. et al. (2020) 'Co-infections in people with COVID-19: a systematic review and meta-analysis', *Jornal of Infections*, 81(January), pp. 266–275. doi: https://doi.org/10.1016/j.jinf.2020.05.046.

Lebreton, F. *et al.* (2021) ' A panel of diverse Pseudomonas aeruginosa clinical isolates for research and development ', *JAC-Antimicrobial Resistance*, 3(4). doi: 10.1093/jacamr/dlab179.

Lee, J. and Zhang, L. (2014) 'The hierarchy quorum sensing network in Pseudomonas aeruginosa', *Protein and Cell*, 6(1), pp. 26–41. doi: 10.1007/s13238-014-0100-x.

Liu, L. P. *et al.* (2019) 'Identification of quorum-sensing molecules of N-acyl-homoserine lactone in Gluconacetobacter strains by liquid chromatography-tandem mass spectrometry', *Molecules*, 24(15). doi: 10.3390/molecules24152694.

Luepke, K. H. *et al.* (2017) 'Past, present, and future of antibacterial economics: increasing bacterial resistance, limited antibiotic pipeline, and societal implications', *pharmacotherapy*, 37, pp. 71–84. doi: 10.1111/j.1875-9114.2016.01868.x.

Luo, J. *et al.* (2017) *Baicalin inhibits biofilm formation, attenuates the quorum sensing-controlled*

virulence and enhances Pseudomonas aeruginosa clearance in a mouse peritoneal implant infection model, *PLoS ONE*. doi: 10.1371/journal.pone.0176883.
Maura, D., Ballok, A. E. and Rahme, L. G. (2016) 'Considerations and caveats in anti-virulence drug development', *Current Opinion in Microbiology*. Elsevier Ltd, 33, pp. 41–46. doi: 10.1016/j.mib.2016.06.001.
Morris, G. M. *et al.* (1998) 'Automated docking using a Lamarckian genetic algorithm and an empirical binding free energy function', *Journal of Computational Chemistry*, 19(14), pp. 1639–1662. doi: 10.1002/(SICI)1096-987X(19981115)19:14<1639::AID-JCC10>3.0.CO;2-B.
Morris, G. M. *et al.* (2009) 'Software news and updates AutoDock4 and AutoDockTools4: Automated docking with selective receptor flexibility', *Journal of Computational Chemistry*, 30(16), pp. 2785–2791. doi: 10.1002/jcc.21256.
Mukherjee, S. *et al.* (2018) 'The PqsE and RhlR proteins are an autoinducer synthase–receptor pair that control virulence and biofilm development in Pseudomonas aeruginosa', *Proceedings of the National Academy of Sciences of the United States of America*, 115(40), pp. E9411–E9418. doi: 10.1073/pnas.1814023115.
Nakano, K. *et al.* (2015) 'First complete genome sequence of Pseudomonas aeruginosa (Schroeter 1872) Migula 1900 (DSM 50071T), determined using PacBio single-molecule real-time technology', *Genome Announcements*, 3(4), pp. 4–5. doi: 10.1128/genomeA.00932-15.
Nassar, O. *et al.* (2022) 'Correlation between phenotypic virulence traits and antibiotic resistance in Pseudomonas aeruginosa clinical isolates', *Microbial Pathogenesis*. Elsevier Ltd, 162(December 2021), p. 105339. doi: 10.1016/j.micpath.2021.105339.
Ni, N. *et al.* (2008) 'Pyrogallol and its analogs can antagonize bacterial quorum sensing in Vibrio harveyi', *Bioorg Med Chem Lett*, 18(5), pp. 1567-72. doi: 10.1016/j.bmcl.2008.01.081.
O'Boyle, N. M. *et al.* (2011) 'Open Babel: An open chemical toolbox', *Journal of Cheminformatics*, 3(33), pp. 1–14. Available at: http://www.jcheminf.com/content/3/1/33%0Ahttp://www.biomedcentral.com/content/pdf/1758-2946-3-33.pdf.
O'Loughlin, C. T. *et al.* (2013) 'A quorum-sensing inhibitor blocks Pseudomonas aeruginosa virulence and biofilm formation', *Proceedings of the National Academy of Sciences of the United States of America*, 110(44), pp. 17981–17986. doi: 10.1073/pnas.1316981110.
O'Reilly, M. C. *et al.* (2018) 'Structural and Biochemical Studies of Non-native Agonists of the LasR Quorum-Sensing Receptor Reveal an L3 Loop "Out" Conformation for LasR', *Cell Chemical Biology*. Elsevier Ltd., 25(9), pp. 1128-1139.e3. doi: 10.1016/j.chembiol.2018.06.007.
Obritsch, M. D. *et al.* (2004) 'National Surveillance of Antimicrobial Resistance in Pseudomonas aeruginosa Isolates Obtained from Intensive Care Unit Patients from 1993 to 2002', 48(12), pp. 4606–4610. doi: 10.1128/AAC.48.12.4606.
Ortori, C. A. *et al.* (2011) 'Simultaneous quantitative profiling of N-acyl-l-homoserine lactone and 2-alkyl-4(1H)-quinolone families of quorum-sensing signaling molecules using LC-MS/MS', *Analytical and Bioanalytical Chemistry*, 399(2), pp. 839–850. doi: 10.1007/s00216-010-4341-0.
Papaioannou, E., Utari, P. D. and Quax, W. J. (2013) 'Choosing an appropriate infection model to study quorum sensing inhibition in Pseudomonas infections', *International Journal of Molecular Sciences*, 14(9), pp. 19309–19340. doi: 10.3390/ijms140919309.
Parasuraman, P. *et al.* (2020) 'Anti-quorum sensing and antibiofilm activities of Blastobotrys parvus PPR3 against Pseudomonas aeruginosa PAO1', *Microbial Pathogenesis*. Elsevier Ltd, 138(October 2019), p. 103811. doi: 10.1016/j.micpath.2019.103811.
Parrinello, M. *et al.* (1981) 'Polymorphic transitions in single crystals: A new molecular dynamics method', *J Applied Physics*, 52(12), pp. 7182–7190. doi:10.1063/1.328693
Pearson, J. P. *et al.* (1994) 'Structure of the autoinducer required for expression of Pseudomonas aeruginosa virulence genes', *Proceedings of the National Academy of Sciences of the United States of*

America, 91(1), pp. 197–201. doi: 10.1073/pnas.91.1.197.
Piepenbrink, K. H. (2020) 'Naringenin Inhibition of the Pseudomonas aeruginosa Quorum Sensing Response Is Based on Its Time-Dependent Competition With N - (3-Oxo-dodecanoyl) - L - homoserine Lactone for LasR Binding', 7(February), pp. 1–11. doi: 10.3389/fmolb.2020.00025.
Proctor, C. R., McCarron, P. A. and Ternan, N. G. (2020) 'Furanone quorum-sensing inhibitors with potential as novel therapeutics against Pseudomonas aeruginosa', *Journal of Medical Microbiology*, 69(2), pp. 195–206. doi: 10.1099/jmm.0.001144.
Pronk, S. et al. (2013) 'GROMACS 4.5: a high-throughput and highly parallel open source molecular simulation toolkit', *Bioinformatics*, 29(7), pp. 845-54. doi: 10.1093/bioinformatics/btt055.
Rasamiravaka, T., Vandeputte, O. M. and El Jaziri, M. (2016) 'Procedure for Rhamnolipids quantification using Methylene-blue', 6, pp. 1–8. doi: 10.21769/BioProtoc.1783.http.
Rawson, T. M. *et al.* (2020) 'Antimicrobial use, drug-resistant infections and COVID-19', *Nature Reviews Microbiology*. Springer US, 18(8), pp. 409–410. doi: 10.1038/s41579-020-0395-y.
Rawson, T. M., Wilson, R. C. and Holmes, A. (2020) 'Understanding the role of bacterial and fungal infection in COVID-19', *Clinical Microbiology and Infection*, 27(January), pp. 9–11. doi: https://doi.org/10.1016/j.cmi.2020.09.025.
Rodighiero, *et al.* (1997) 'Synthesis and biological properties of some 2H-1-benzopyrano[7,8-b][1,4]benzodioxin-2-ones', *Farmaco*, 52(1), pp. 7-12.
Roudashti, S. *et al.* (2017) 'Synergistic activity of sub-inhibitory concentrations of curcumin with ceftazidime and ciprofloxacin against Pseudomonas aeruginosa quorum sensing related genes and virulence traits', *World Journal of Microbiology and Biotechnology*. Springer Netherlands, 33(3), p. 0. doi: 10.1007/s11274-016-2195-0.
Ruffin, M. *et al.* (2016) 'Quorum-sensing inhibition abrogates the deleterious impact of Pseudomonas aeruginosa on airway epithelial repair', *FASEB Journal*, 30(9), pp. 3011–3025. doi: 10.1096/fj.201500166R.
Sar, B. *et al.* (1999) 'Induction of interleukin 8 (IL-8) production by Pseudomonas nitrite reductase in human alveolar macrophages and epithelial cells', *Microbiology and Immunology*, 43(5), pp. 409–417. doi: 10.1111/j.1348-0421.1999.tb02424.x.
Soukarieh, F. *et al.* (2018) 'Pseudomonas aeruginosa Quorum Sensing Systems as Drug Discovery Targets: Current Position and Future Perspectives', *Journal of Medicinal Chemistry*, 61(23), pp. 10385–10402. doi: 10.1021/acs.jmedchem.8b00540.
Sriramulu, D. D. *et al.* (2005) 'Microcolony formation: A novel biofilm model of Pseudomonas aeruginosa for the cystic fibrosis lung', *Journal of Medical Microbiology*, 54(7), pp. 667–676. doi: 10.1099/jmm.0.45969-0.
Strateva, T. and Mitov, I. (2011) 'Contribution of an arsenal of virulence factors to pathogenesis of Pseudomonas aeruginosa infections', *Annals of Microbiology*, 61(4), pp. 717–732. doi: 10.1007/s13213-011-0273-y.
Teplitski, M. *et al.* (2004) 'Chlamydomonas reinhardtii secretes compounds that mimic bacterial signals and interfere with quorum sensing regulation in bacteria', *Plant* Physiol, 134(1), pp. 137-146. doi: 10.1104/pp.103.029918.
Thi, M. T. T., Wibowo, D. and Rehm, B. H. A. (2020) 'Pseudomonas aeruginosa biofilms', *International Journal of Molecular Sciences*, 21(22), pp. 1–25. doi: 10.3390/ijms21228671.
Topa, S. H. *et al.* (2020) 'Activity of Cinnamaldehyde on Quorum Sensing and Biofilm Susceptibility to Antibiotics in Pseudomonas aeruginosa', *Microorganisms*, 8(3).
Tsai, C. J. Y., Loh, J. M. S. and Proft, T. (2016) 'Galleria mellonella infection models for the study of bacterial diseases and for antimicrobial drug testing', *Virulence*. Taylor & Francis, 7(3), pp. 214–229. doi: 10.1080/21505594.2015.1135289.
Turkina, M. V. and Vikström, E. (2019) 'Bacteria-Host Crosstalk: Sensing of the Quorum in the Context of Pseudomonas aeruginosa Infections', *Journal of Innate Immunity*, 11(3), pp. 263–279. doi:

10.1159/000494069.
Ugurlu, A. *et al.* (2016) 'Phenolic compounds affect production of pyocyanin, swarming motility and biofilm formation of Pseudomonas aeruginosa', *Asian Pacific Journal of Tropical Biomedicine*. Elsevier B.V., 6(8), pp. 698–701. doi: 10.1016/j.apjtb.2016.06.008.
Van der Spoel, D. *et al*., (2005) 'GROMACS: fast, flexible, and free', *J Comput Chem*, 26(16), pp. 1701-18. doi: 10.1002/jcc.20291
Vanommeslaeghe, K. *et al.* (2012) 'Automation of the CHARMM General Force Field (CGenFF) I: bond perception and atom typing', *J Chem Inf Model*, 52(12), pp. 3144-54. doi: 10.1021/ci300363c.
Vincent, J.-L. (1995) 'The Prevalence of Nosocomial Infection in Intensive Care Units in Europe', *Jama*, 274(8), p. 639. doi: 10.1001/jama.1995.03530080055041.
Viradi, M. *et al*. (2022) 'AlphaFold Protein Structure Database: massively expanding the structural coverage of protein-sequence space with high-accuracy models', *Nucleic Acids Res*, 50(D1), pp. D439-D444. doi: 10.1093/nar/gkab1061.
Wagner, V. E. *et al.* (2006) 'Quorum sensing: Dynamic response of Pseudomonas aeruginosa to external signals', *Trends in Microbiology*, 14(2), pp. 55–58. doi: 10.1016/j.tim.2005.12.002.
Walsh, D. J. *et al.* (2019) 'Antimicrobial Activity of Naturally Occurring Phenols and Derivatives Against Biofilm and Planktonic Bacteria', *Frontiers in Chemistry*, 7(October), pp. 1–13. doi: 10.3389/fchem.2019.00653.
Waters, CM. et al., (2006) 'The Vibrio harveyi quorum-sensing system uses shared regulatory components to discriminate between multiple autoinducers', *Genes Dev*, 20(19), pp. 2754-67. doi: 10.1101/gad.1466506
Yang, D. *et al.* (2021) 'Paeonol Attenuates Quorum-Sensing Regulated Virulence and Biofilm Formation in Pseudomonas aeruginosa', *Frontiers in Microbiology*, 12(August). doi: 10.3389/fmicb.2021.692474.
Yin, H. *et al.* (2015) 'Tea polyphenols as an antivirulence compound Disrupt Quorum-Sensing Regulated Pathogenicity of Pseudomonas aeruginosa', *Sci Rep*, 5, pp. 16158. doi: 10.1038/srep16158
Zhu, J. *et al*. (1998) 'Analogs of the autoinducer 3-oxooctanoyl-homoserine lactone strongly inhibit activity of the TraR protein of *Agrobacterium tumefaciens*', *J Bacteriol*, 180(20), pp. 5398-405. doi: 10.1128/JB.180.20.5398-5405.1998.

9 Figure and legends

Figure 1. Effect of compounds selected by bioluminescence assay on the expression of AHL-sensitive genes. (A) Heatmap illustrating differential gene expression over vehicle-treated controls. PAO1 (10^6 CFU/mL) cultures were treated with 100µM of compounds GM-14, GM-22, GM-24, GM-30, GM-42, GM-43, GM-50, GM-79 or with vehicle (DMSO 0.05%) for 24 hrs at 37 °C. Transcript levels of AHL-responsive genes *lasR/lasI/lasB* and *rhlR/rhlI/rhlA*, were assessed by qRT-PCR. Expression values for each gene (rows) are normalized across all samples (columns) by proC expression. Positive correlations are marked in red and negative ones in blue (color scale at top). **(B)** Chemical structures of GM-22, GM-50, and GM-79. **(C)** PAO1 (10^6 CFU/mL) were cultured in LB with GM-50 (10, 50, and 100 µM). After 24 hrs, *LasR/lasI/lasB* and *rhlR/rhlI/rhlA* mRNA transcript levels were determined by qRT-PCR. Results are reported as $2^{\Delta\Delta Ct}$ of relative gene expression (n=3). *p<0.05, **p<0.01 vs PAO1 with DMSO 0.05%.

Figure 2. Effect of GM-50 on prokaryotic and eukaryotic cells growth and viability. PAO1 (10^6 CFU/mL) cultures were treated with 100 µM of GM-50 or vehicle. **(A)** Bacterial growth was monitored

for 36 hrs by measuring optical density (OD=620 nm). **(B)** Bacterial viability was evaluated by seeding proper culture dilutions in LB agar and enumerating colonies (CFU) after 16 hrs (n=3) **(C)** Human respiratory tract epithelial cells A549 were cultured with GM-50 at concentrations ranging from 0 to 10 mM. Cell viability was assessed by MTT (3-(4,5-dimethylthiazol-2-yL)-2,5- diphenyltetrazolium bromide) assay. Data (*n*=3) are reported as percent cell viability calculated over the control (vehicle).

Figure 3. Effect of GM-50 on AHL production. PAO1 (10^6 CFU/mL) were cultured in LB with GM-50 (100µM) or DMSO 0.05% (vehicle) for 24 hrs at 37 °C. After incubation, supernatants were used to quantify AHL production adopting LC-MS technology using both reverse phase chromatography and luminescence assay. **(A)** LC-MS chromatogram of collected supernatants. C6HSL (*m/z* 200), 3-Oxo-C9-HSL (*m/z* 256), N-decanoyl-homoserine lactone (m/z 256), 3-Oxo-10-HSL N-dodecanoyl-homoserine lactone (*m/z* 270), 3-oxo-C12-HSL (*m/z* 284), 3-Oxo-C12-HSL isomer 1 and 2 (*m/z* 298) were detected. **(B)** Total quantification of AHL molecules is reported as µg/mL. **(C)** Supernatants were added to *Vibrio harveyi* BB120. Luminescence was quantified after 24 hrs. Results obtained with PAO1 cultured with DMSO were arbitrarily assigned 100% AHL production. *p<0.05, **p<0.01 *vs* PAO1 with DMSO 0.05%.

Figure 4. Effect of GM-50 on PA01 virulence factors expression. PAO1 (10^6 CFU/mL) was cultured in LB with GM-50 (100µM) or DMSO 0.05% (vehicle) for 24 hrs at 37 °C. After incubation, supernatants were used to quantify **(A)** pyocyanin production by chloroform-HCl method, **(C)** elastase production by Elastin-Congo red assay, **(D)** rhamnolipids release by methylene blue staining. **(B** and **E)** Transcript levels of *phzA* and *rhlA*, genes involved in pyocyanin and rhamnolipids production respectively, were assessed by qRT-PCR. **(F)** To evaluate swarming, PAO1 cultures were inoculated on the center of LB-agar plates (0.5% agar) and incubated at 37 °C. We then evaluated the distance from the center. PAO1 + DMSO 0,05% was used as positive control and was arbitrarily set at 100%. **(G)** PAO1 (10^6 CFU/mL) was cultured in ASM for 24 hrs at 37 °C with moderate agitation (75 rpm) to form biofilm. PAO1 mature biofilm was treated with aztreonam (Abx, 4 µg/mL), GM-50 (100µM), or aztreonam (Abx, antibiotic) and GM-50 for 16 hrs. Residual biofilm was then evaluated by measuring the relative fluorescence units (RFU) using a fluorimeter (Ex = 530–570 nm, Em = 590–620 nm). Data are reported as the percentage of biofilm calculated by setting DMSO as 100%. Data are represented as mean ± SEM, n = 3 experiments. *p<0.05, **p<0.01, ***p<0.001, ****p<0.0001 vs PAO1 with DMSO 0.05%. **(H)** Schematic representation of the experimental design for biofilm evaluation reported in **G**.

Figure 5. Effect of GM-50 on PA01-epithelial cells interaction and PAO1 *G. mellonella in-vivo* infection model. PAO1 (10^6 CFU/mL) was cultured in LB with GM-50 (100µM) or DMSO 0.05% (vehicle) for 24 hrs at 37 °C and used to infect adherent A549 cells monolayers (MOI 1:20) for 2 hrs. **(A** and **B)** cells were washed, and cultured for 24hrs in fresh DMEM containing gentamycin sulfate (200 µg/mL). IL-8 and IL-6 were quantified by ELISA in conditioned media. **(C)** cells were washed, collected, lysed, seeded on LB-agar plates, and incubated overnight at 37 °C to enumerate total bacteria associated with A549 monolayers (internalized and adherent) expressed as CFU/cell. **(D)** Cells were washed and incubated in media containing gentamycin sulfate. After 2 hrs cells were washed, collected, lysed, and seeded on LB-agar plates to enumerate internalized bacteria, expressed as CFU/cell. Data are represented as mean ± SEM, n = 3 experiments. *p<0.05, **p<0.01, ***p<0.001, ****p<0.0001 vs PAO1 with DMSO 0.05%. **(E)** Schematic representation of the experimental design. *G. mellonella*

larvae were infected with 10 CFU of PAO1. Two hrs later, larvae were injected into the right proleg with specified compounds and monitored for 40 hrs. **(F)** Kaplan-Meier survival curve of infected *G. mellonella* receiving no treatment, treatment with GM-50 or GM-32, a molecule devoid of activity on AHL-dependent QS (see Supplementary Materials). *p<0.05 vs PAO1. **(G)** Average hrs of larvae survival post-infection.

Figure 6. Effect of GM-50 on virulence factors expression in *P. aeruginosa* clinical isolates. *P. aeruginosa* respiratory tract isolates were cultured (10^6 CFU/mL) in LB with GM-50 (100µM) or DMSO 0.05% (vehicle) for 24 hrs at 37 °C. After incubation, supernatants were used to quantify elastase release by Elastin-Congo red assay or pyocyanin production by the chloroform-HCl method. Pyocyanin and elastase obtained with strains cultured with DMSO 0.05% were arbitrarily assigned 100% production and were used as control. Data are represented as mean±SEM, n = 3 experiments for each clinical isolate. ***p<0.001 *vs* control.

Figure 7. Molecular docking simulations. Root mean square deviation (RMSD) values were obtained during the first 10 ns of molecular dynamics simulations. **(A)** RMSD values for the LasR C-alpha atoms (blue line) and GM-50 (displacement of ligand heavy atoms with respect to protein C-alpha atoms; red line). **(B)** RMSD values for the RhlI C-alpha atoms (blue line) and GM-50 (displacement of ligand heavy atoms with respect to protein C-alpha atoms; red line). **(C)** RMSD values for the LasI C-alpha atoms (blue line) and GM-50 (displacement of ligand heavy atoms with respect to protein C-alpha atoms; red line). In all the cases, while the proteins resulted stable during the simulations, the ligand was readily displaced from the binding site (RMSD > 0.6 nm within 10 ns).

Figure 8. Results of molecular docking and molecular dynamics simulations between GM-50 and RhlR. (A) Predicted interactions between GM-50 and RhlR. H-bonds and π-π interactions are depicted as dashed red lines. **(B)** Root-mean squared deviation (RMSD) values for the protein C-alpha atoms (blue line) and GM-50 (displacement of ligand heavy atoms with respect to protein C-alpha atoms; red line). **(C)** Time dependent distance between GM-50 phenolic function and 81Asp sidechain (blue line) and between GM-50 phenolic function and 68Trp indole NH (red line). Both the distances are compatible with stable H-bonds. **(D)** Time dependent interaction energies (Kcal/mol) between GM-50 and RhlR (red line) and between C4HSL and RhlR (blue line).

Figure 9. Schematic illustration of QS in *P. aeruginosa* and effects of GM-50. (A) Representation rhl quorum-sensing system in *P. aeruginosa*. After a threshold concentration of signal molecule C4HSL, the C4HSL-RhlR complex binds the promoter regions of responsive genes, activating or repressing their transcription. C4HSL-RhlR complex induces lasI expression, enhancing the production of C4HSL (autoinduction effect). Among virulence factors regulated by this pathway are genes involved in biofilm formation, pyocyanin and rhamnolipids release, elastase production, and swarming motility. **(B)** Compound GM-50 competes with C4HSL for the binding to the specific receptor, thus reducing the expression of *P. aeruginosa* virulence genes even in the presence of autoinducers in the environment.

10. Tables

Table 1: Oligonucleotides sequences and annealing conditions used in the qRT-PCR experiments.

Gene	Primers used for qRT-PCR	Annealing temp (°C)
***proC* (HK)**	fw 5'- CAGGCCGGGCAGTTGCTGTC -3'	60°C
	rv 5'- GGTCAGGCGCGAGGCTGTCT -3'	
lasI	fw 5'- GGCTGGGACGTTAGTGTCAT -3'	60°C
	rv 5'- AAAACCTGGGCTTCAGGAGT -3'	
lasR	fw 5'- ACGCTCAAGTGGAAAATTGG -3'	60°C
	rv 5'-TCGTAGTCCTGGCTGTCCTT -5'	
rhlI	fw 5'- AAGGACGTCTTCGCCTACCT -3'	60°C
	rv 5'- GCAGGCTGGACCAGAATATC -3'	
rhlR	fw 5'- CATCCGATGCTGATGTCCAACC-3'	60°C
	rv 5'- ATGATGGCGATTTCCCCGGAAC -3'	
lasB	fw 5'-GACCGAGAATGACAAAGTGGAA -3'	60°C
	rv 5'- GGTAGGAGACGTTGTAGACCAGTTG -3'	
rhlA	fw 5'- TGGCCGAACATTTCAACGT -3'	60°C
	rv 5'- GATTTCCACCTCGTCGTCCTT -3'	
phzA	fw 5' – CGAGGATCCGAACCACTTCT -3'	60°C
	rv 5' – AACGGCTATTCCCAATGCAC -3'	

1035

Figure 1.TIF

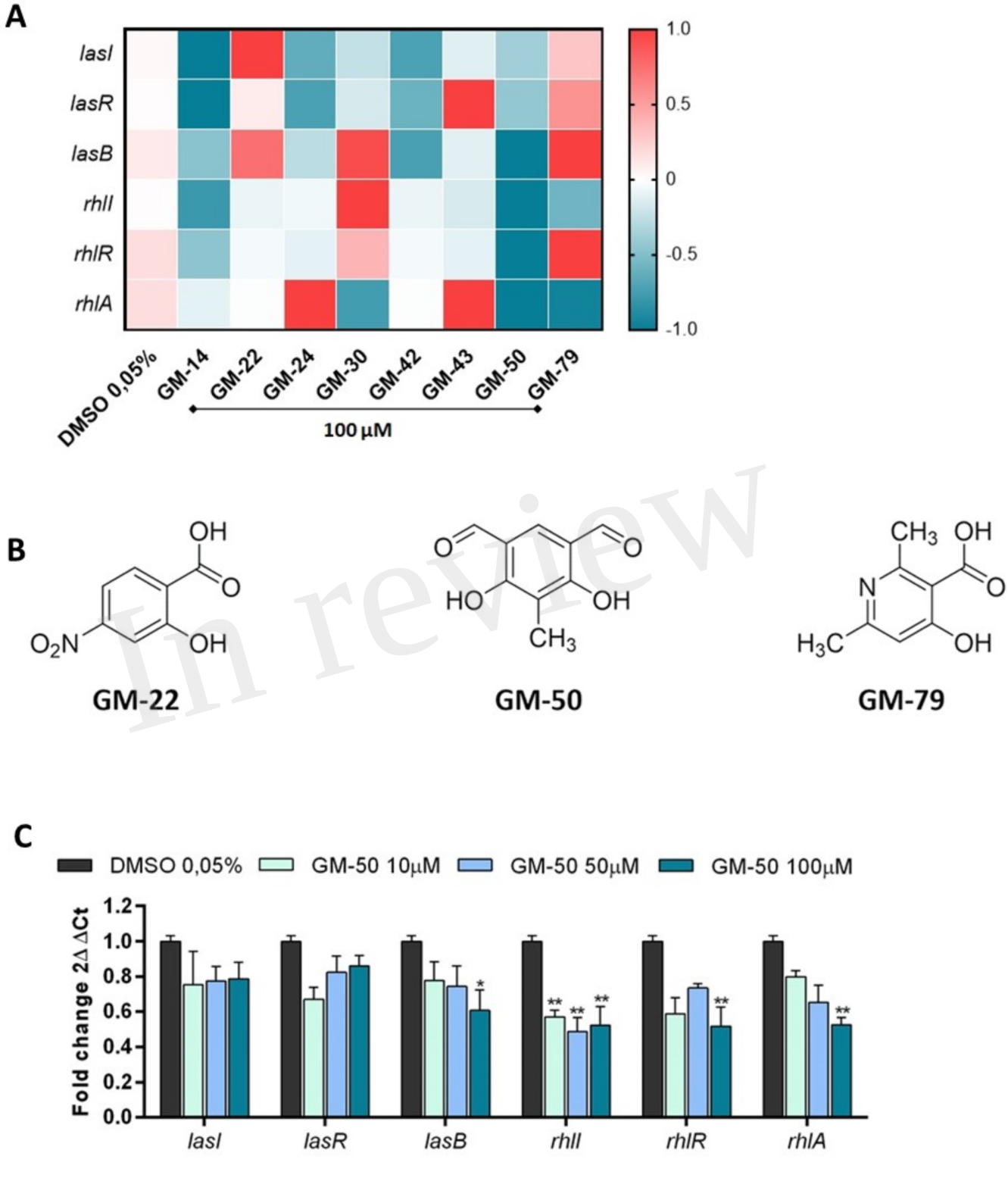

Figure 2.TIF

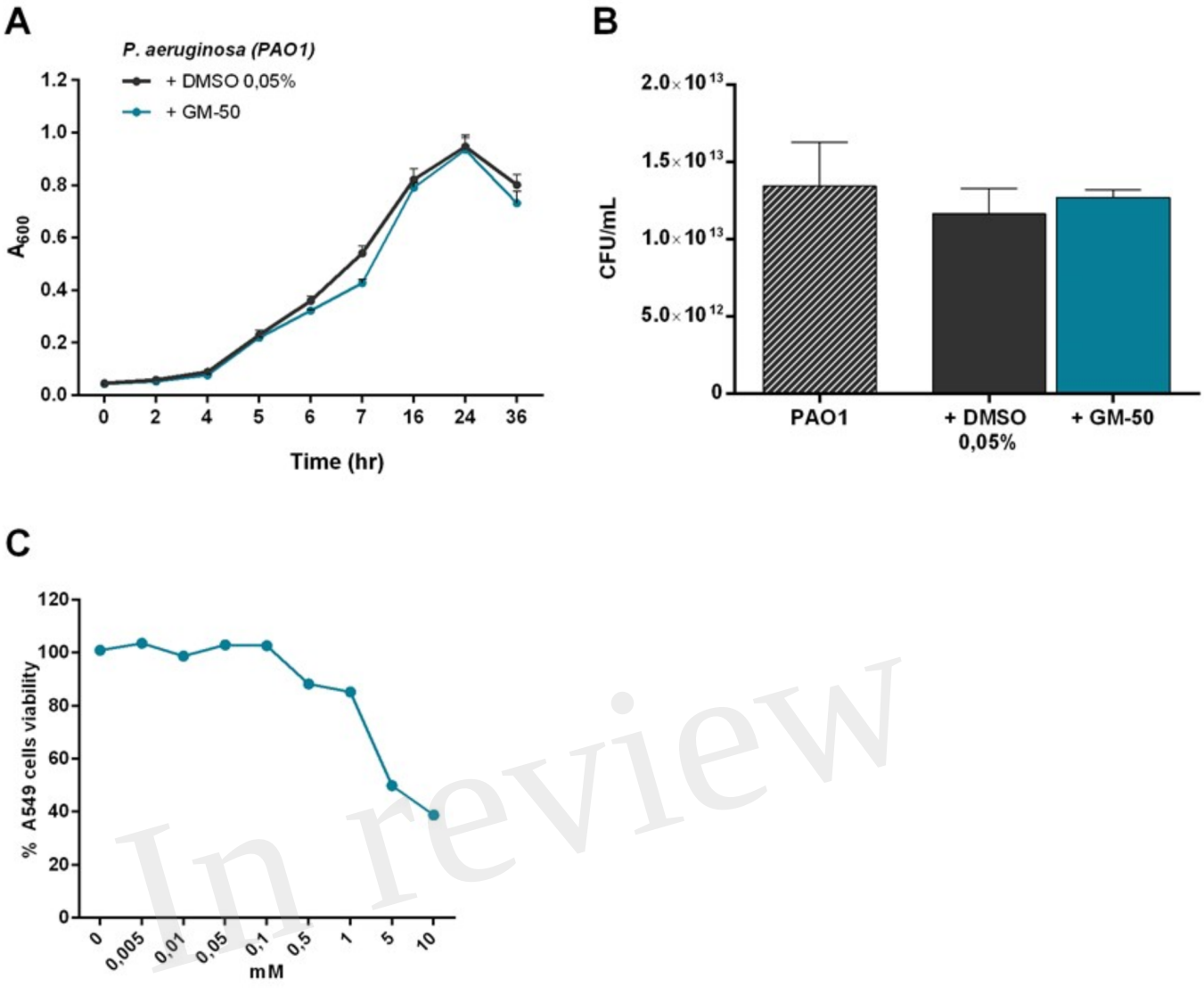

Figure 3.TIF

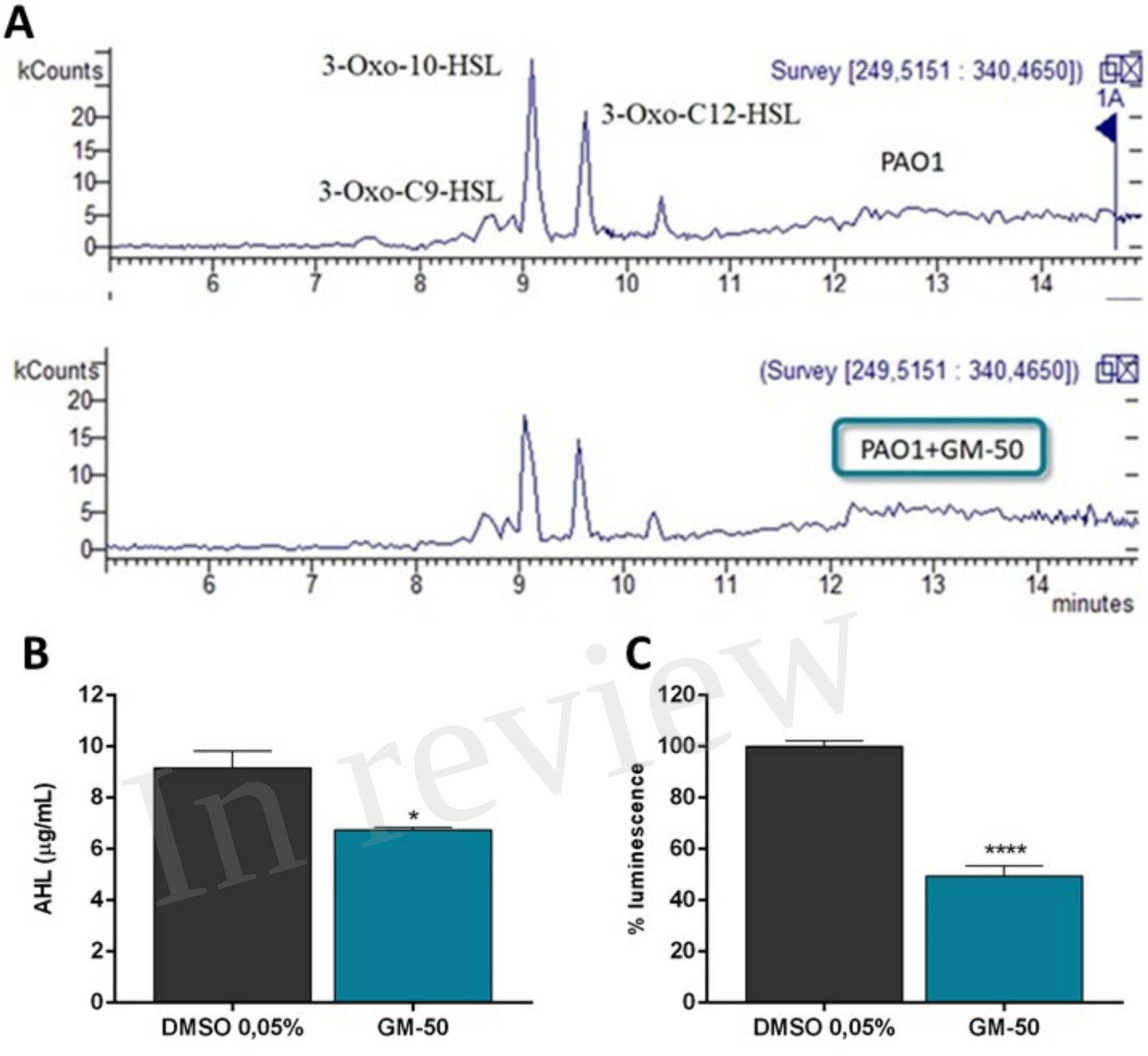

Figure 4.TIF

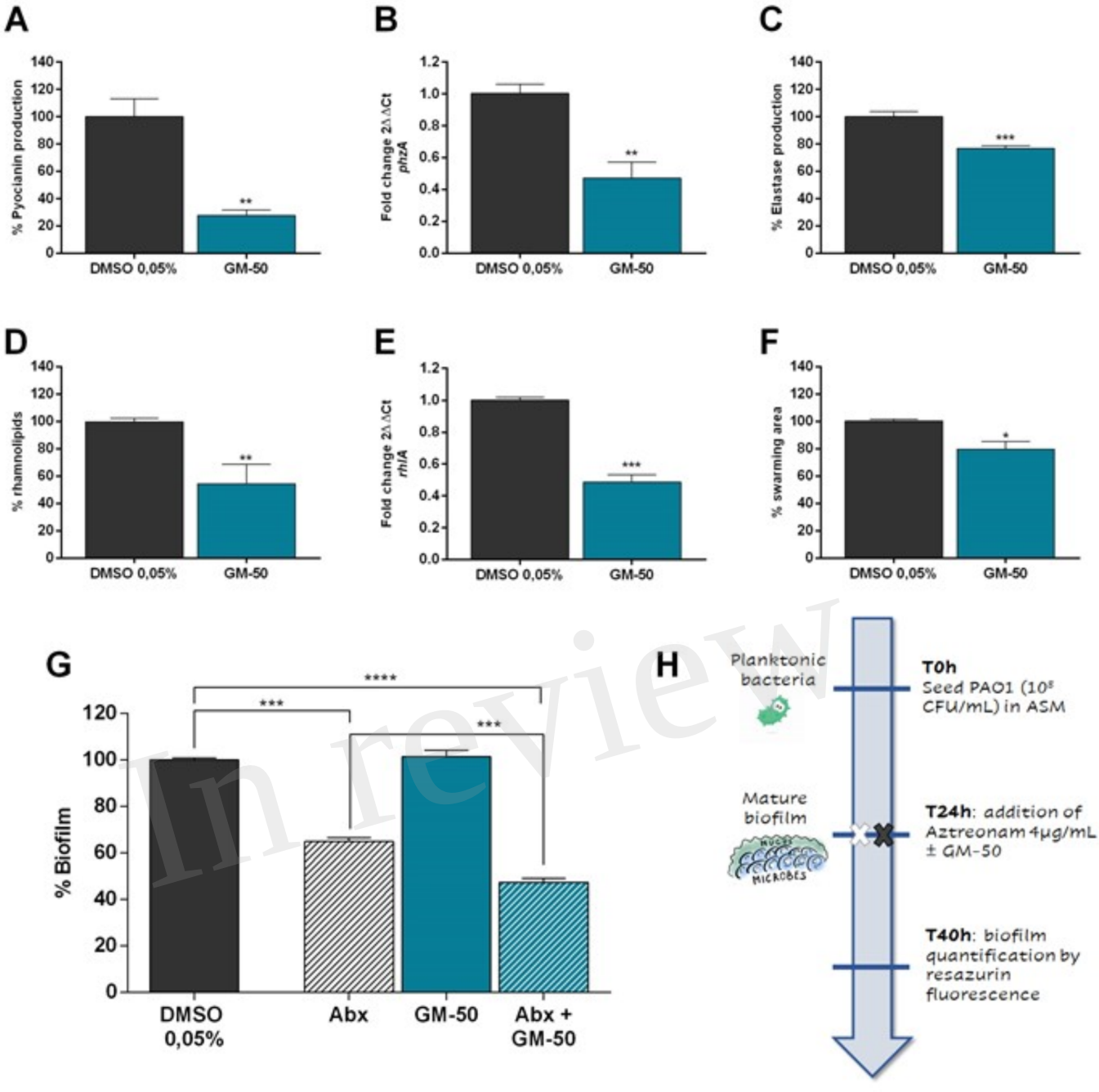

Figure 5.TIF

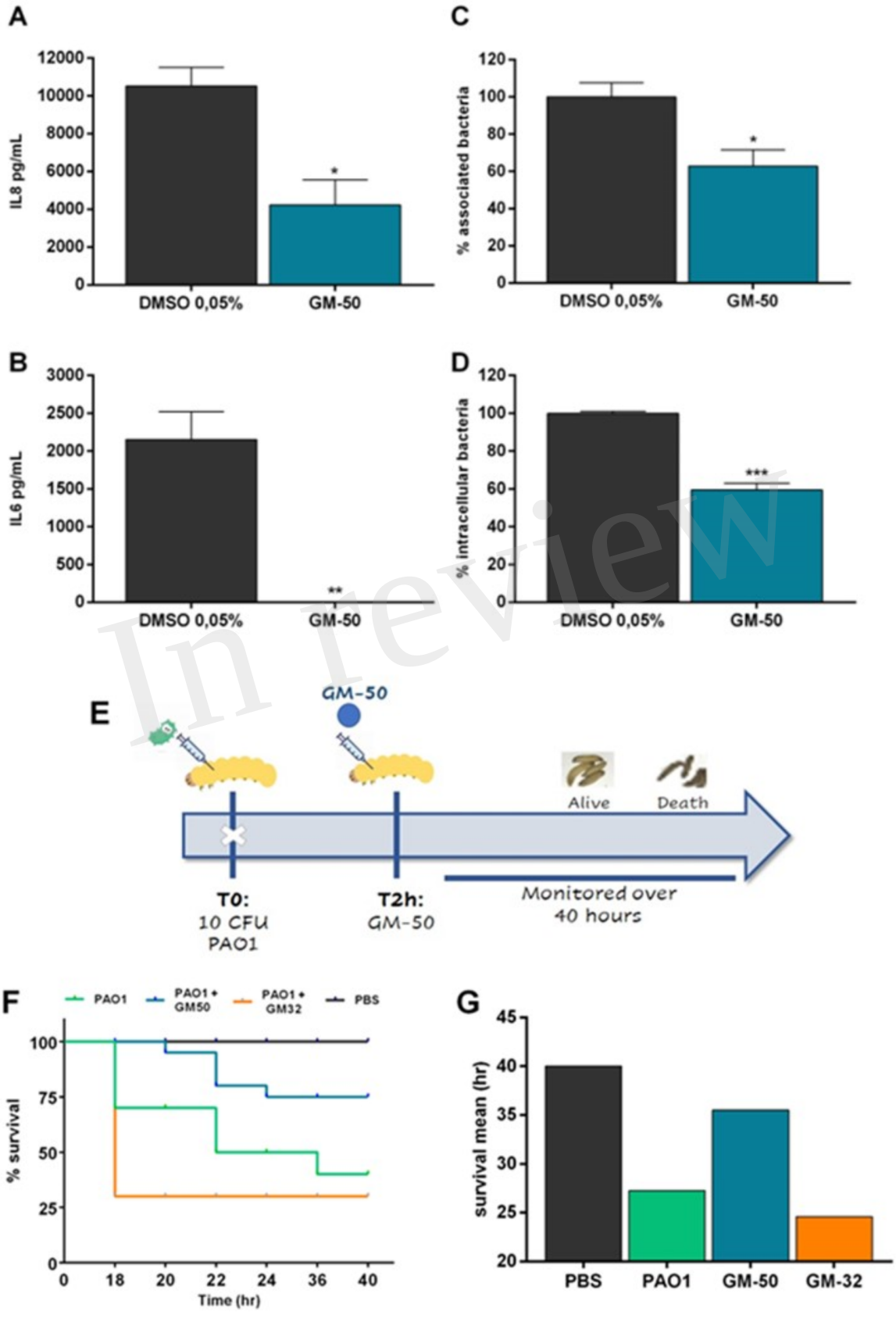

Figure 6.TIF

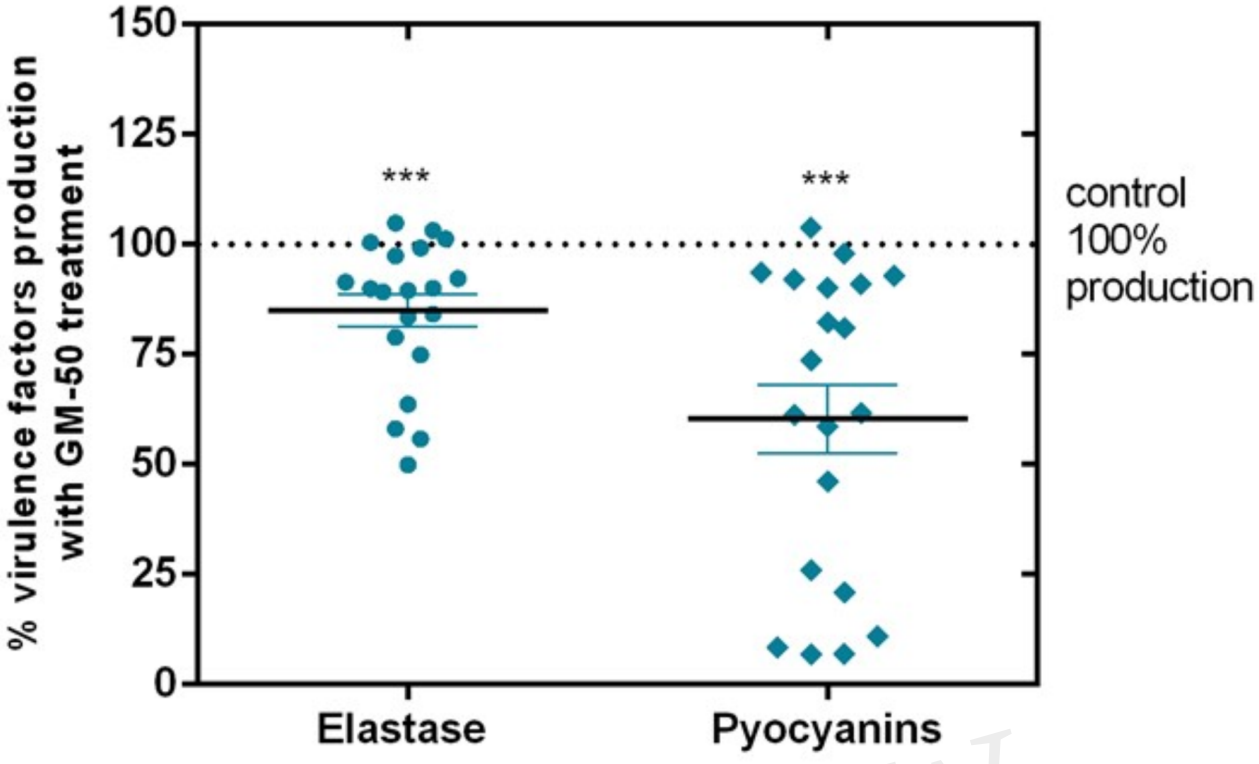

Figure 7.TIF

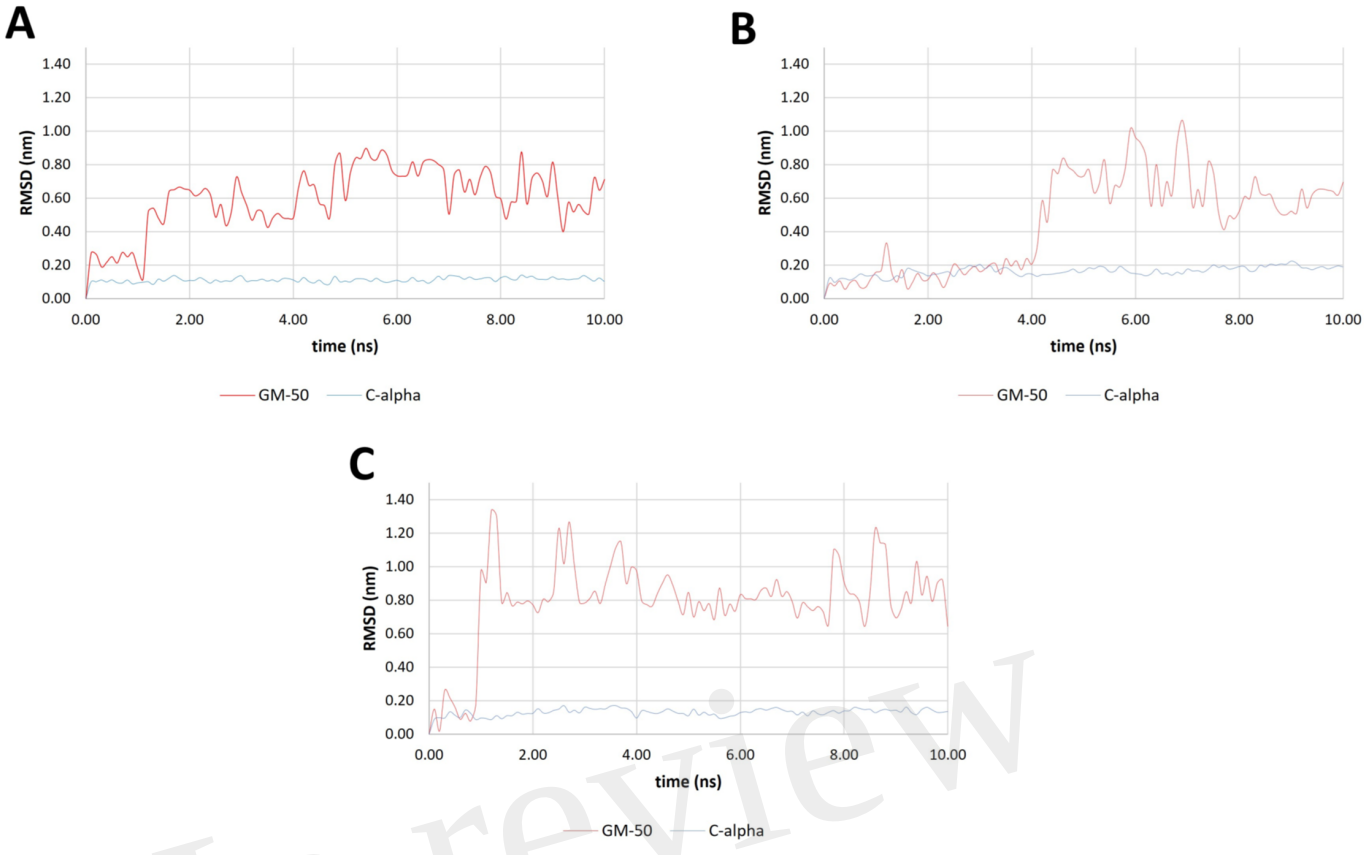

Figure 8.TIF

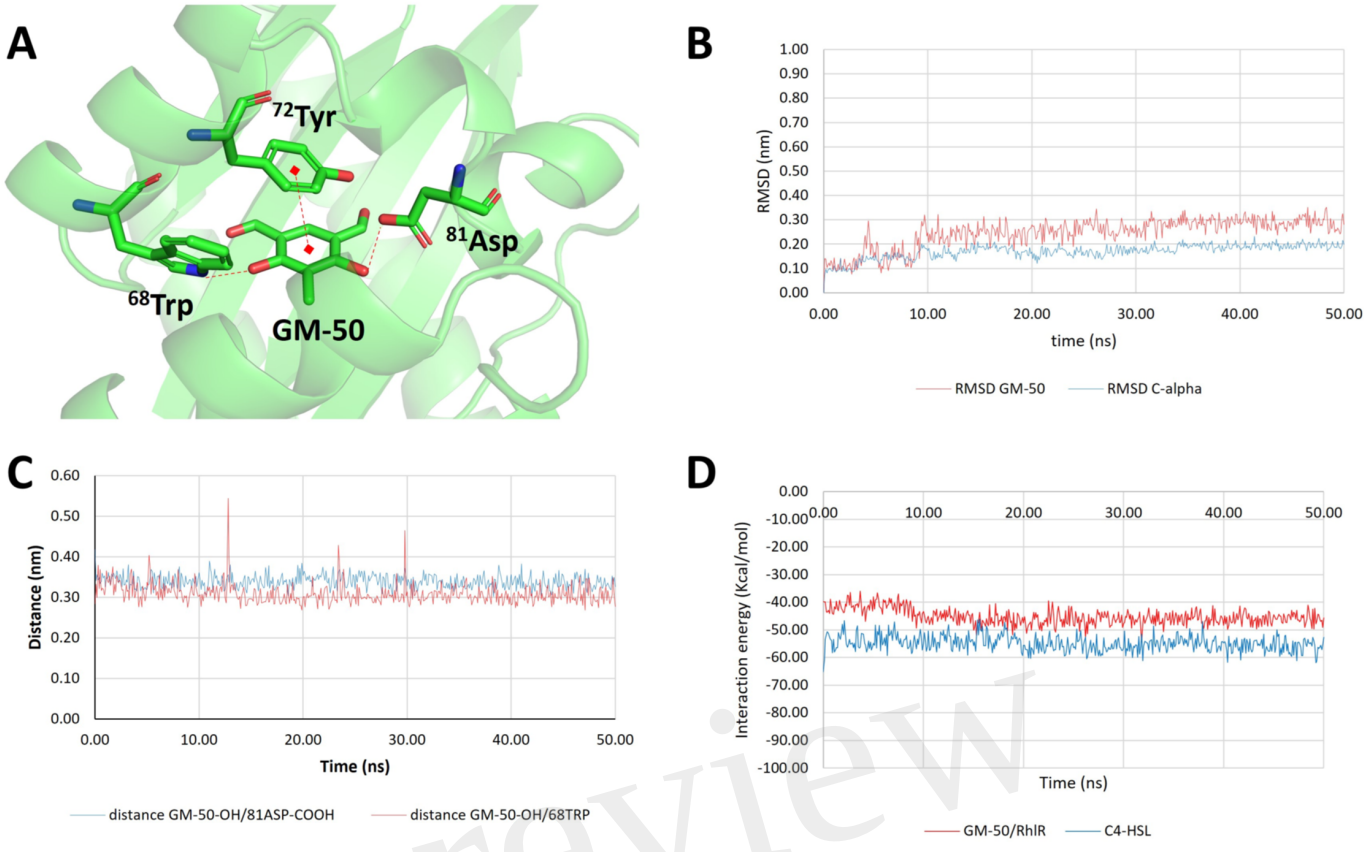

Figure 9.TIF